

Towards Realistic Susy Spectra and Yukawa Textures from Intersecting Branes

Ching-Ming Chen,¹ Tianjun Li,^{1,2} V.E. Mayes,¹ and D.V. Nanopoulos^{1,3}¹*George P. and Cynthia W. Mitchell Institute for Fundamental Physics, Texas A&M University,
College Station, TX 77843, USA*²*Institute of Theoretical Physics, Chinese Academy of Sciences, Beijing 100080, China*³*Astroparticle Physics Group, Houston Advanced Research Center (HARC),
Mitchell Campus, Woodlands, TX 77381, USA;
Academy of Athens, Division of Natural Sciences,
28 Panepistimiou Avenue, Athens 10679, Greece*

ABSTRACT

We study the possible phenomenology of a three-family Pati-Salam model constructed from intersecting D6-branes in Type IIA string theory on the $\mathbf{T}^6/(\mathbb{Z}_2 \times \mathbb{Z}_2)$ orientifold with some desirable semi-realistic features. In the model, tree-level gauge coupling unification is achieved automatically at the string scale, and the gauge symmetry may be broken to the Standard Model (SM) close to the string scale. The small number of extra chiral exotic states in the model may be decoupled via the Higgs mechanism and strong dynamics. We calculate the possible supersymmetry breaking soft terms and the corresponding low-energy supersymmetric particle spectra which may potentially be tested at the Large Hadron Collider (LHC). We find that for the viable regions of the parameter space the lightest CP-even Higgs boson mass usually satisfies $m_H \leq 120$ GeV, and the observed dark matter density may be generated. Finally, we find that it is possible to obtain correct SM quark masses and mixings, and the tau lepton mass at the unification scale. Additionally, neutrino masses and mixings may be generated via the seesaw mechanism. Mechanisms to stabilize the open and closed-string moduli, which are necessary for the model to be truly viable and to make definite predictions are discussed.

I. INTRODUCTION

Although string theory has long teased us with her power to encompass all known physical phenomena in a complete mathematical structure, an actual worked out example is still lacking. Indeed, the major problem of string phenomenology is to construct *at least one* realistic model with all moduli stabilized, which completely describes known particle physics as well as potentially being predictive of unknown phenomena. With the dawn of the Large Hadron Collider (LHC) era, new discoveries will hopefully be upon us. In particular, supersymmetry is expected to be found as well as the Higgs states required to break the electroweak symmetry. Therefore, it is highly desirable to have complete, concrete models derived from string theory which are able to make predictions for the superpartner spectra, as well as describing currently known particle physics.

In the old days of string phenomenology, model builders were primarily focused on weakly coupled heterotic string theory. However, with the advent of the second string revolution, D-branes [1] have created new interest in Type I and II compactifications. In particular, Type IIA orientifolds with intersecting D6-branes, where the chiral fermions arise at the intersections of D6-branes in the internal space [2], with T-dual Type IIB description in terms of magnetized D-branes [3], have shown great promise during the last few years. Indeed, intersecting D-brane configurations provide promising setups which may accommodate semi-realistic features of low-energy physics. Given this, it is an interesting question to see how far one can get from a particular string compactification to reproducing the finer details of the Standard Model as a low-energy effective field theory.

In order to construct globally consistent vacua with intersecting D-branes, conditions must be imposed which strongly constrain the models. In particular, all Ramond-Ramond (RR) tadpoles must be cancelled and K-theory [4] conditions for cancelling the nontrivial Z_2 anomaly also must be imposed. Despite the clear benefits of supersymmetry, there have been many three-family standard-like models and Grand Unified Theories (GUT) constructed on Type IIA orientifolds [5, 6, 7] which are not supersymmetric. Although these models are globally consistent, they are generally plagued by the gauge hierarchy problem and vacuum instability which arises from uncanceled Neveu-Schwarz-Neveu-Schwarz (NSNS) tadpoles. Later, semi-realistic supersymmetric Standard-like, Pati-Salam, unflipped $SU(5)$ as well as flipped $SU(5)$ models in Type IIA theory on $\mathbf{T}^6/(\mathbb{Z}_2 \times \mathbb{Z}_2)$ [8, 9, 10, 11, 12, 13, 14, 15] and $\mathbf{T}^6/(\mathbb{Z}_2 \times \mathbb{Z}_2')$ [16, 17, 18] orientifolds were eventually constructed, and some of their phenomenological consequences studied [19, 20]. Other supersymmetric constructions in Type IIA theory on different orientifold backgrounds have also

been discussed [21]. Nonperturbative D-instanton effects have also been receiving much attention of late, and may play an important role [22] [23] [24] [25].

In addition to satisfying the above consistency conditions, all open and closed-string moduli must be stabilized in order to obtain an actual vacuum. Unstabilized moduli are manifest in the low-energy theory as massless scalar fields, which are clearly in conflict with observations. Given a concrete string model, the low-energy observables such as particle couplings and resulting masses are functions of the open and closed string moduli. In a fully realistic model, these moduli must therefore be stabilized and given sufficiently large masses to meet the astrophysical/cosmological and collider physics constraints on additional scalar fields. Although satisfying the conditions for $\mathcal{N} = 1$ supersymmetry in Type IIA (IIB) fixes the complex structure (Kähler) moduli in these models, the Kähler (complex structure) and open-string moduli generally remain unfixed. To stabilize some of these moduli, supergravity three-form fluxes [26] and geometric fluxes [27] were introduced and flux models on Type II orientifolds have been constructed [28, 29, 30, 31, 32, 33, 34, 35, 36, 37]. Models where the D-branes wrap rigid cycles, thus freezing the open-string moduli have also been studied [16, 17, 18].

Despite substantial progress, there have been other roadblocks in constructing phenomenologically realistic intersecting D-brane models, besides the usual problem of moduli stabilization. Unlike heterotic models, the gauge couplings are not automatically unified. Additionally, there has been a rank one problem in the Standard Model (SM) fermion Yukawa matrices, preventing the generation of mass for the first two generations of quarks and leptons. For the case of toroidal orientifold compactifications, this can be traced to the fact that not all of the Standard Model fermions are localized at intersections on the same torus. However, one example of an intersecting D6-brane model on Type IIA $\mathbf{T}^6/(\mathbb{Z}_2 \times \mathbb{Z}_2)$ orientifold has recently been discovered where these problems may be solved [12, 36]. Thus, this particular model may be a step forward to obtaining realistic phenomenology from string theory. Indeed, as we recently discussed [38], it is possible within the moduli space of this model to obtain correct quark mass matrices and mixings, the tau lepton mass, and to generate naturally small neutrino masses via the seesaw mechanism. Furthermore, it is possible to generically study the soft supersymmetry breaking terms, from which can be calculated the supersymmetric partner spectra, the Higgs masses, and the resulting neutralino relic density.

This paper is organized as follows. First, we will briefly review the intersecting D6-brane model on Type IIA $\mathbf{T}^6/(\mathbb{Z}_2 \times \mathbb{Z}_2)$ orientifold which we are studying and discuss its basic features. We then discuss the low-energy effective action, and show that the tree-level gauge couplings are unified

near the string scale. We also find that the hidden sector gauge groups will become confining at a high energy scale, thus decoupling chiral exotics present in the model. Next, we study the possible low-energy superpartner spectra which may arise. We also calculate the Yukawa couplings for quarks and leptons in this model, and show that we may obtain the correct quark masses and mixings and the tau lepton mass for specific choices of the open and closed string-moduli VEVs. We should emphasize that for the present work, we will not focus on the moduli stabilization problem, as our goal is only to explore the possible phenomenological characteristics of the model. However, we do comment on this issue and discuss how it may potentially be solved for this model. We also should note that models with an equivalent observable sector have been constructed in Type IIA and Type IIB theory as Ads and Minkowski flux vacua [36, 39], so that the issue of closed-string moduli stabilization has already been addressed to some extent.

II. A D-BRANE MODEL WITH DESIRABLE SEMI-REALISTIC FEATURES

In recent years, intersecting D-brane models have provided an exciting approach towards constructing semi-realistic vacua. To summarize, D6 branes (in Type IIA) fill three-dimensional Minkowski space and wrap 3-cycles in the compactified manifold, with a stack of N branes having a gauge group $U(N)$ (or $U(N/2)$ in the case of $T^6/(\mathbb{Z}_2 \times \mathbb{Z}_2)$) in its world volume. The 3-cycles wrapped by the D-branes will in general intersect multiple times in the internal space, resulting in a chiral fermion in the bifundamental representation localized at the intersection between different stacks. The multiplicity of such fermions is then given by the number of times the 3-cycles intersect. Due to orientifolding, for every stack of D6-branes we must also introduce its orientifold images. Thus, the D6-branes may also have intersections with the images of other stacks, also resulting in fermions in bifundamental representations. Each stack may also intersect its own images, resulting in chiral fermions in the symmetric and antisymmetric representations. The different types of representations that may be obtained for each type of intersection and their multiplicities are shown in Table I. In addition, there are constraints that must be satisfied for the consistency of the model, namely the requirement for Ramond-Ramond tadpole cancellation and to have a spectrum with $\mathcal{N} = 1$ supersymmetry.

Intersecting D-brane configurations provide promising setups which may accommodate semi-realistic features of low-energy physics. Given this, it is an interesting question to see how far one can get from a particular string compactification to reproducing the finer details of the Standard Model as a low-energy effective field theory. There have been many consistent models studied,

but only a small number have the proper structures to produce an acceptable phenomenology. A good candidate for a realistic model which may possess the proper structures was discussed in [12, 36, 38] in Type IIA theory on the $\mathbf{T}^6/(\mathbb{Z}_2 \times \mathbb{Z}_2)$ orientifold. This background has been extensively studied and we refer the reader to [8, 9] for reviews of the basic model building rules. We present the D6-brane configurations and intersection numbers of this model in Table II, and the resulting spectrum which is essentially that of a three-family Pati-Salam in Table III [12, 36]. We put the a' , b , and c stacks of D6-branes on the top of each other on the third two torus, and as a result there are additional vector-like particles from $N = 2$ subsectors.

TABLE I: General spectrum for intersecting D6-branes at generic angles, where $I_{aa'} = -2^{3-k} \prod_{i=1}^3 (n_a^i l_a^i)$, and $I_{aO6} = 2^{3-k} (-l_a^1 l_a^2 l_a^3 + l_a^1 n_a^2 n_a^3 + n_a^1 l_a^2 n_a^3 + n_a^1 n_a^2 l_a^3)$. Moreover, \mathcal{M} is the multiplicity, and a_S and a_A denote the symmetric and anti-symmetric representations of $U(N_a/2)$, respectively.

Sector	Representation
aa	$U(N_a/2)$ vector multiplet and 3 adjoint chiral multiplets
$ab + ba$	$\mathcal{M}(\frac{N_a}{2}, \frac{N_b}{2}) = I_{ab} = 2^{-k} \prod_{i=1}^3 (n_a^i l_b^i - n_b^i l_a^i)$
$ab' + b'a$	$\mathcal{M}(\frac{N_a}{2}, \frac{N_b}{2}) = I_{ab'} = -2^{-k} \prod_{i=1}^3 (n_a^i l_b^i + n_b^i l_a^i)$
$aa' + a'a$	$\mathcal{M}(a_S) = \frac{1}{2}(I_{aa'} - \frac{1}{2}I_{aO6})$; $\mathcal{M}(a_A) = \frac{1}{2}(I_{aa'} + \frac{1}{2}I_{aO6})$

The anomalies from three global $U(1)$ s of $U(4)_C$, $U(2)_L$ and $U(2)_R$ are cancelled by the Green-Schwarz mechanism, and the gauge fields of these $U(1)$ s obtain masses via the linear $B \wedge F$ couplings. Thus, the effective gauge symmetry is $SU(4)_C \times SU(2)_L \times SU(2)_R$. In order to break the gauge symmetry, on the first torus, we split the a stack of D6-branes into a_1 and a_2 stacks with 6 and 2 D6-branes, respectively, and split the c stack of D6-branes into c_1 and c_2 stacks with two D6-branes for each one, as shown in Figure 1. In this way, the gauge symmetry is further broken to $SU(3)_C \times SU(2)_L \times U(1)_{I_{3R}} \times U(1)_{B-L}$. Moreover, the $U(1)_{I_{3R}} \times U(1)_{B-L}$ gauge symmetry may be broken to $U(1)_Y$ by giving vacuum expectation values (VEVs) to the vector-like particles with the quantum numbers $(\mathbf{1}, \mathbf{1}, \mathbf{1}/2, -1)$ and $(\mathbf{1}, \mathbf{1}, -\mathbf{1}/2, 1)$ under the $SU(3)_C \times SU(2)_L \times U(1)_{I_{3R}} \times U(1)_{B-L}$ gauge symmetry from $a_2 c'_1$ intersections [12, 36].

Since the gauge couplings in the Minimal Supersymmetric Standard Model (MSSM) are unified at the GUT scale $\sim 2.4 \times 10^{16}$ GeV, the additional exotic particles present in the model must necessarily become superheavy. To accomplish this it is first assumed that the $USp(2)_1$ and

TABLE II: D6-brane configurations and intersection numbers for the model on Type IIA $\mathbf{T}^6/\mathbb{Z}_2 \times \mathbb{Z}_2$ orientifold. The complete gauge symmetry is $[U(4)_C \times U(2)_L \times U(2)_R]_{\text{observable}} \times [USp(2)^4]_{\text{hidden}}$, the SM fermions and Higgs fields arise from the intersections on the first two-torus, and the complex structure parameters are $2\chi_1 = 6\chi_2 = 3\chi_3 = 6$.

$U(4)_C \times U(2)_L \times U(2)_R \times USp(2)^4$													
	N	$(n^1, l^1) \times (n^2, l^2) \times (n^3, l^3)$	n_S	n_A	b	b'	c	c'	1	2	3	4	
a	8	$(0, -1) \times (1, 1) \times (1, 1)$	0	0	3	0	-3	0	1	-1	0	0	
b	4	$(3, 1) \times (1, 0) \times (1, -1)$	2	-2	-	-	0	0	0	1	0	-3	
c	4	$(3, -1) \times (0, 1) \times (1, -1)$	-2	2	-	-	-	-1	0	3	0		
1	2	$(1, 0) \times (1, 0) \times (2, 0)$	$\chi_1 = 3, \chi_2 = 1, \chi_3 = 2$										
2	2	$(1, 0) \times (0, -1) \times (0, 2)$	$\beta_1^g = -3, \beta_2^g = -3$										
3	2	$(0, -1) \times (1, 0) \times (0, 2)$	$\beta_3^g = -3, \beta_4^g = -3$										
4	2	$(0, -1) \times (0, 1) \times (2, 0)$											

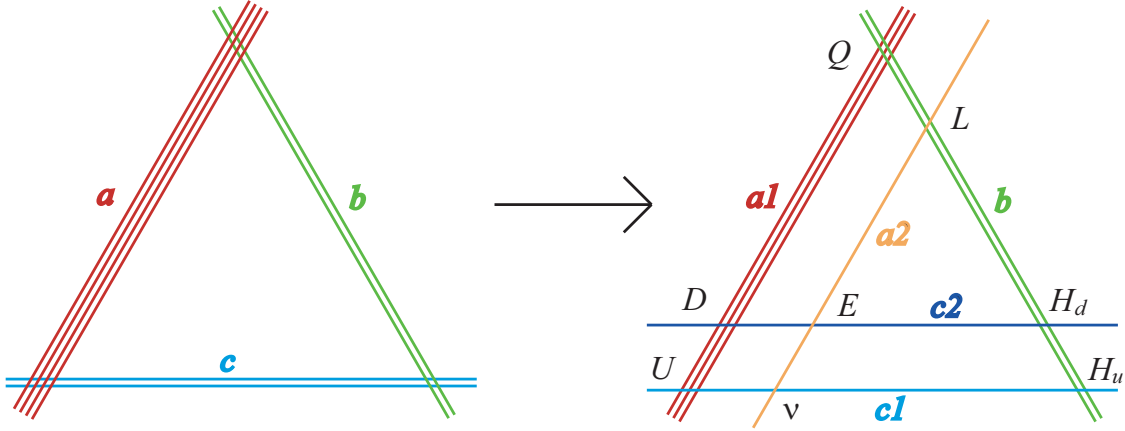


FIG. 1: Breaking of the effective gauge symmetry $SU(4) \times SU(2)_L \times SU(2)_R$ down to $SU(3)_C \times U(2)_L \times U(1)_{I3R} \times U(1)_{B-L}$ via brane splitting. This process corresponds to giving a VEV to adjoint scalars, which arise as open-string moduli associated with the positions of stacks a and c in the internal space.

$USp(2)_2$ stacks of D6-branes lie on the top of each other on the first torus, so we have two pairs of vector-like particles X_{12}^i with $USp(2)_1 \times USp(2)_2$ quantum numbers $(2, 2)$. These particles can break $USp(2)_1 \times USp(2)_2$ down to the diagonal $USp(2)_{D12}$ near the string scale by obtaining VEVs, and then states arising from intersections $a1$ and $a2$ may obtain vector-like masses close to the string scale from superpotential terms of the form

$$W \subset X_{a1} X_{a2} X_{12}^i, \quad (1)$$

TABLE III: The chiral and vector-like superfields, and their quantum numbers under the gauge symmetry $SU(4)_C \times SU(2)_L \times SU(2)_R \times USp(2)_1 \times USp(2)_2 \times USp(2)_3 \times USp(2)_4$.

	Quantum Number	Q_4	Q_{2L}	Q_{2R}	Field
ab	$3 \times (4, \bar{2}, 1, 1, 1, 1, 1)$	1	-1	0	$F_L(Q_L, L_L)$
ac	$3 \times (\bar{4}, 1, 2, 1, 1, 1, 1)$	-1	0	1	$F_R(Q_R, L_R)$
$a1$	$1 \times (4, 1, 1, 2, 1, 1, 1)$	1	0	0	X_{a1}
$a2$	$1 \times (\bar{4}, 1, 1, 1, 2, 1, 1)$	-1	0	0	X_{a2}
$b2$	$1 \times (1, 2, 1, 1, 2, 1, 1)$	0	1	0	X_{b2}
$b4$	$3 \times (1, \bar{2}, 1, 1, 1, 1, 2)$	0	-1	0	X_{b4}^i
$c1$	$1 \times (1, 1, \bar{2}, 2, 1, 1, 1)$	0	0	-1	X_{c1}
$c3$	$3 \times (1, 1, 2, 1, 1, 2, 1)$	0	0	1	X_{c3}^i
b_S	$2 \times (1, 3, 1, 1, 1, 1, 1)$	0	2	0	T_L^i
b_A	$2 \times (1, \bar{1}, 1, 1, 1, 1, 1)$	0	-2	0	S_L^i
c_S	$2 \times (1, 1, \bar{3}, 1, 1, 1, 1)$	0	0	-2	T_R^i
c_A	$2 \times (1, 1, 1, 1, 1, 1, 1)$	0	0	2	S_R^i
ab'	$3 \times (4, 2, 1, 1, 1, 1, 1)$	1	1	0	
	$3 \times (\bar{4}, \bar{2}, 1, 1, 1, 1, 1)$	-1	-1	0	
ac'	$3 \times (4, 1, 2, 1, 1, 1, 1)$	1		1	Φ_i
	$3 \times (\bar{4}, 1, \bar{2}, 1, 1, 1, 1)$	-1	0	-1	$\bar{\Phi}_i$
bc	$6 \times (1, 2, \bar{2}, 1, 1, 1, 1)$	0	1	-1	H_u^i, H_d^i
	$6 \times (1, \bar{2}, 2, 1, 1, 1, 1)$	0	-1	1	

where we neglect the couplings of order one. Moreover, we assume that the T_R^i and S_R^i obtain VEVs near the string scale, and their VEVs satisfy the D-flatness of $U(1)_R$. We also assume that there exist various suitable high-dimensional operators in the effective theory, and thus the adjoint chiral superfields may obtain GUT-scale masses via these operators. With T_R^i and S_R^i , we can give GUT-scale masses to the particles from the intersections $c1$, $c3$, and c_S via the supepotential:

$$W \subset S_R^i X_{c1} X_{c1} + T_R^i X_{c3}^j X_{c3}^k + \frac{1}{M_{Pl}} S_R^i S_R^j T_R^k T_R^l. \quad (2)$$

The beta function for $USp(2)_{D12}$ is -4 and the gauge coupling for $USp(2)_{D12}$ will become strongly coupled around 5×10^{12} GeV, and then we can give 5×10^{12} GeV scale VEVs to S_L^i and preserve the D-flatness of $U(1)_L$. The remaining states may also obtain intermediate scale masses via the operators

$$W \subset X_{b2} X_{b2} S_L^i + \frac{X_{b2} X_{b2}}{M_X} X_{b4} X_{b4}. \quad (3)$$

To have one pair of light Higgs doublets, it is necessary to fine-tune the mixing parameters of the Higgs doublets. In particular, the μ term and the right-handed neutrino masses may be generated via the following high-dimensional operators

$$W \supset \frac{y_{\mu}^{ijkl}}{M_{\text{St}}} S_L^i S_R^j H_u^k H_d^l + \frac{y_{Nij}^{mnkl}}{M_{\text{St}}^3} T_R^m T_R^n \Phi_i \Phi_j F_R^k F_R^l, \quad (4)$$

where y_{μ}^{ijkl} and y_{Nij}^{mnkl} are Yukawa couplings, and M_{St} is the string scale. Thus, the μ term is TeV scale and the right-handed neutrino masses can be in the range 10^{10-14} GeV for $y_{\mu}^{ijkl} \sim 1$ and $y_{Nij}^{mnkl} \sim 10^{(-7)-(-3)}$.

III. THE $\mathcal{N} = 1$ LOW-ENERGY EFFECTIVE ACTION

In building a concrete string model which may be testable, it is not enough to simply reproduce the matter and gauge symmetry of the known low-energy particle states in the Standard Model. It is also necessary to make predictions regarding the superpartner spectra and Higgs masses. If supersymmetry exists as expected and is softly broken, then it is possible to calculate the soft SUSY breaking terms, which determine the low energy sparticle spectra. Furthermore, if the neutralino is the lightest supersymmetric particle (LSP), then it is expected to make up a large fraction of the observed dark matter density, $0.0945 < \Omega h^2 < 0.1287$ at 2σ [40, 41], and this is calculable from the soft terms. Ideally, one would also like to be able to calculate the Yukawa couplings for the known quarks and leptons, and be able to reproduce their masses and mixings.

To discuss the low-energy phenomenology we start from the low-energy effective action. From the effective scalar potential it is possible to study the stability [42], the tree-level gauge couplings [19, 43, 44], gauge threshold corrections [45], and gauge coupling unification [46]. The effective Yukawa couplings [47, 48], matter field Kähler metric and soft-SUSY breaking terms have also been investigated [49]. A more detailed discussion of the Kähler metric and string scattering of gauge, matter, and moduli fields has been performed in [50]. Although turning on Type IIB 3-form fluxes can break supersymmetry from the closed string sector [28, 29, 30, 31, 32, 33], there are additional terms in the superpotential generated by the fluxes and there is currently no satisfactory model which incorporates this. Thus, we do not consider this option in the present work. In principle, it should be possible to specify the exact mechanism by which supersymmetry is broken, and thus to make very specific predictions. However, for the present work, we will adopt a parametrization of the SUSY breaking so that we can study it generically.

The $\mathcal{N} = 1$ supergravity action depends upon three functions, the holomorphic gauge kinetic

function, f , Kähler potential K , and the superpotential W . Each of these will in turn depend upon the moduli fields which describe the background upon which the model is constructed. The holomorphic gauge kinetic function for a D6-brane wrapping a calibrated three-cycle is given by [34]

$$f_P = \frac{1}{2\pi\ell_s^3} \left[e^{-\phi} \int_{\Pi_P} \text{Re}(e^{-i\theta_P} \Omega_3) - i \int_{\Pi_P} C_3 \right]. \quad (5)$$

In terms of the three-cycle wrapped by the stack of branes, we have

$$\int_{\Pi_a} \Omega_3 = \frac{1}{4} \prod_{i=1}^3 (n_a^i R_1^i + 2^{-\beta_i} i l_a^i R_2^i). \quad (6)$$

from which it follows that

$$f_P = \frac{1}{4\kappa_P} (n_P^1 n_P^2 n_P^3 s - \frac{n_P^1 l_P^2 l_P^3 u^1}{2^{(\beta_2+\beta_3)}} - \frac{n_P^2 l_P^1 l_P^3 u^2}{2^{(\beta_1+\beta_3)}} - \frac{n_P^3 l_P^1 l_P^2 u^3}{2^{(\beta_1+\beta_2)}}), \quad (7)$$

where $\kappa_P = 1$ for $SU(N_P)$ and $\kappa_P = 2$ for $USp(2N_P)$ or $SO(2N_P)$ gauge groups and where we use the s and u moduli in the supergravity basis. In the string theory basis, we have the dilaton S , three Kähler moduli T^i , and three complex structure moduli U^i [50]. These are related to the corresponding moduli in the supergravity basis by

$$\begin{aligned} \text{Re}(s) &= \frac{e^{-\phi_4}}{2\pi} \left(\frac{\sqrt{\text{Im } U^1 \text{Im } U^2 \text{Im } U^3}}{|U^1 U^2 U^3|} \right) \\ \text{Re}(u^j) &= \frac{e^{-\phi_4}}{2\pi} \left(\sqrt{\frac{\text{Im } U^j}{\text{Im } U^k \text{Im } U^l}} \right) \left| \frac{U^k U^l}{U^j} \right| \quad (j, k, l) = (\overline{1}, 2, 3) \\ \text{Re}(t^j) &= \frac{i\alpha'}{T^j} \end{aligned} \quad (8)$$

and ϕ_4 is the four-dimensional dilaton. To second order in the string matter fields, the Kähler potential is given by

$$K(M, \bar{M}, C, \bar{C}) = \hat{K}(M, \bar{M}) + \sum_{\text{untwisted } i,j} \tilde{K}_{C_i \bar{C}_j}(M, \bar{M}) C_i \bar{C}_j + \sum_{\text{twisted } \theta} \tilde{K}_{C_\theta \bar{C}_\theta}(M, \bar{M}) C_\theta \bar{C}_\theta. \quad (9)$$

The untwisted moduli C_i , \bar{C}_j are light, non-chiral scalars from the field theory point of view, associated with the D-brane positions and Wilson lines. These fields are not observed in the MSSM, and if they were present in the low energy spectra may disrupt the gauge coupling unification. Clearly, these fields must get a large mass through some mechanism. One way to accomplish this is to require the D-branes to wrap rigid cycles, which freezes the open string moduli [17]. However, there are no rigid cycles available on $T^6/(\mathbb{Z}_2 \times \mathbb{Z}_2)$ without discrete torsion, thus we will assume that the open-string moduli become massive via high-dimensional operators.

For twisted moduli arising from strings stretching between stacks P and Q , we have $\sum_j \theta_{PQ}^j = 0$, where $\theta_{PQ}^j = \theta_Q^j - \theta_P^j$ is the angle between the cycles wrapped by the stacks of branes P and Q on the j^{th} torus respectively. Then, for the Kähler metric in Type IIA theory we find the following two cases:

- $\theta_{PQ}^j < 0, \theta_{PQ}^k > 0, \theta_{PQ}^l > 0$

$$\begin{aligned} \tilde{K}_{PQ} = & e^{\phi_4} e^{\gamma_E(2 - \sum_{j=1}^3 \theta_{PQ}^j)} \sqrt{\frac{\Gamma(\theta_{PQ}^j)}{\Gamma(1 + \theta_{PQ}^j)}} \sqrt{\frac{\Gamma(1 - \theta_{PQ}^k)}{\Gamma(\theta_{PQ}^k)}} \sqrt{\frac{\Gamma(1 - \theta_{PQ}^l)}{\Gamma(\theta_{PQ}^l)}} \\ & (t^j + \bar{t}^j)^{\theta_{PQ}^j} (t^k + \bar{t}^k)^{-1 + \theta_{PQ}^k} (t^l + \bar{t}^l)^{-1 + \theta_{PQ}^l}. \end{aligned} \quad (10)$$

- $\theta_{PQ}^j < 0, \theta_{PQ}^k < 0, \theta_{PQ}^l > 0$

$$\begin{aligned} \tilde{K}_{PQ} = & e^{\phi_4} e^{\gamma_E(2 + \sum_{j=1}^3 \theta_{PQ}^j)} \sqrt{\frac{\Gamma(1 + \theta_{PQ}^j)}{\Gamma(-\theta_{PQ}^j)}} \sqrt{\frac{\Gamma(1 + \theta_{PQ}^k)}{\Gamma(-\theta_{PQ}^k)}} \sqrt{\frac{\Gamma(\theta_{PQ}^l)}{\Gamma(1 - \theta_{PQ}^l)}} \\ & (t^j + \bar{t}^j)^{-1 - \theta_{PQ}^j} (t^k + \bar{t}^k)^{-1 - \theta_{PQ}^k} (t^l + \bar{t}^l)^{-\theta_{PQ}^l}. \end{aligned} \quad (11)$$

For branes which are parallel on at least one torus, giving rise to non-chiral matter in bifundamental representations (for example, the Higgs doublets), the Kähler metric is

$$\hat{K} = ((s + \bar{s})(t^1 + \bar{t}^1)(t^2 + \bar{t}^2)(u^3 + \bar{u}^3))^{-1/2}. \quad (12)$$

The superpotential is given by

$$W = \hat{W} + \frac{1}{2} \mu_{\alpha\beta}(M) C^\alpha C^\beta + \frac{1}{6} Y(M)_{\alpha\beta\gamma} C^{\alpha\beta\gamma} + \dots \quad (13)$$

while the minimum of the F part of the tree-level supergravity scalar potential V is given by

$$V(M, \bar{M}) = e^G (G_M K^{MN} G_N - 3) = (F^N K_{NM} F^M - 3e^G), \quad (14)$$

where $G_M = \partial_M G$ and $K_{NM} = \partial_N \partial_M K$, K^{MN} is inverse of K_{NM} , and the auxiliary fields F^M are given by

$$F^M = e^{G/2} K^{ML} G_L. \quad (15)$$

Supersymmetry is broken when some of the F-terms of the hidden sector fields M acquire VEVs. This then results in soft terms being generated in the observable sector. For simplicity, it is assumed

in this analysis that the D -term does not contribute (see [51]) to the SUSY breaking. Then the goldstino is included by the gravitino via the superHiggs effect. The gravitino then obtains a mass

$$m_{3/2} = e^{G/2}, \quad (16)$$

which we will take to be ≈ 1 TeV in the following. The normalized gaugino mass parameters, scalar mass-squared parameters, and trilinear parameters respectively may be given in terms of the Kähler potential, the gauge kinetic function, and the superpotential as

$$\begin{aligned} M_P &= \frac{1}{2\text{Re}f_P}(F^M \partial_M f_P), \\ m_{PQ}^2 &= (m_{3/2}^2 + V_0) - \sum_{M,N} \bar{F}^{\bar{M}} F^N \partial_{\bar{M}} \partial_N \log(\tilde{K}_{PQ}), \\ A_{PQR} &= F^M \left[\hat{K}_M + \partial_M \log(Y_{PQR}) - \partial_M \log(\tilde{K}_{PQ} \tilde{K}_{QR} \tilde{K}_{RP}) \right], \end{aligned} \quad (17)$$

where \hat{K}_M is the Kähler metric appropriate for branes which are parallel on at least one torus, i.e. involving non-chiral matter.

The above formulas for the soft terms depend on the Yukawa couplings, via the superpotential. An important consideration is whether or not this should cause any modification to the low-energy spectrum. However, this turns out not to be the case since the Yukawas in the soft term formulas are not the same as the physical Yukawas, which arise from world-sheet instantons and are proportional to $\exp(-A)$, where A is the world-sheet area of the triangles formed by a triplet of intersections at which the Standard Model fields are localized. As we shall see in a later section, the physical Yukawa couplings in Type IIA depend on the Kähler moduli and the open-string moduli. This ensures that the Yukawa couplings present in the soft terms do not depend on either the complex-structure moduli or dilaton (in the supergravity basis). Thus, the Yukawa couplings will not affect the low-energy spectrum in the case of u -moduli dominant and mixed u and s dominant supersymmetry breaking.

To determine the SUSY soft breaking parameters, and therefore the spectra of the models, we introduce the VEVs of the auxiliary fields Eq. (15) for the dilaton, complex and Kähler moduli [52]:

$$\begin{aligned} F^s &= 2\sqrt{3}Cm_{3/2}\text{Re}(s)\Theta_s e^{-i\gamma_s}, \\ F^{\{u,t\}^i} &= 2\sqrt{3}Cm_{3/2}(\text{Re}(u^i)\Theta_i^u e^{-i\gamma_i^u} + \text{Re}(t^i)\Theta_i^t e^{-i\gamma_i^t}). \end{aligned} \quad (18)$$

The factors γ_s and γ_i are the CP violating phases of the moduli, while the constant C is given by

$$C^2 = 1 + \frac{V_0}{3m_{3/2}^2}. \quad (19)$$

The goldstino is included in the gravitino by Θ_S in S field space, and Θ_i parameterize the goldstino direction in U^i space, where $\sum(|\Theta_i^u|^2 + |\Theta_i^t|^2) + |\Theta_s|^2 = 1$. The goldstino angle Θ_s determines the degree to which SUSY breaking is being dominated by the dilaton s and/or complex structure (u^i) and Kähler (t^i) moduli. As suggested earlier, we will not consider the case of t -moduli dominant supersymmetry breaking as in this case, the soft terms are not independent of the Yukawa couplings.

IV. GAUGE COUPLING UNIFICATION

The MSSM predicts the unification of the three gauge couplings at an energy $\sim 2.4 \times 10^{16}$ GeV. In intersecting D-brane models, the gauge groups arise from different stacks of branes, and so they will not generally have the same volume in the compactified space. Thus, the gauge couplings are not automatically unified, in contrast to heterotic models. For branes wrapping cycles not invariant under ΩR , the holomorphic gauge kinetic function for a D6 brane stack P is given by Eq. (7). where u^i and s are the complex structure moduli and dilaton in the supergravity basis.

The gauge coupling constant associated with a stack P is given by

$$g_{D6_P}^{-2} = |\text{Re}(f_P)|. \quad (20)$$

Thus, for the model under study the $SU(3)$ holomorphic gauge function is identified with stack $a1$ and the $SU(2)$ holomorphic gauge function with stack b . The Q_Y holomorphic gauge function is then given by taking a linear combination of the holomorphic gauge functions from all the stacks. Note that we have absorbed a factor of $1/2$ in the definition of Q_Y so that the electric charge is given by $Q_{em} = T_3 + Q_Y$. In this way, it is found [53] that

$$f_Y = \frac{1}{6}f_{a1} + \frac{1}{2}f_{a2} + \frac{1}{2}f_{c1} + \frac{1}{2}f_{c2}. \quad (21)$$

Recalling that the complex structure moduli U^i are obtained from the supersymmetry conditions, we have for the present model

$$U^1 = 3i, \quad U^2 = i, \quad U^3 = -1 + i. \quad (22)$$

Thus, we find that the tree-level MSSM gauge couplings will be automatically unified at the string scale

$$g_s^2 = g_w^2 = \frac{5}{3}g_Y^2 = \left[\frac{e^{-\phi_4}}{2\pi} \frac{\sqrt{6}}{4} \right]^{-1}. \quad (23)$$

Even though the gauge couplings are unified, this does not fix the actual value of the couplings as these still depend upon the value taken by the four-dimensional dilaton ϕ_4 . In order for the gauge

couplings to have the value observed for the MSSM ($g_{\text{unification}}^2 \approx 0.511$), we must choose $\phi_4 = -3$ such that $e^{-\phi_4} \approx 20$, which fixes the string scale as

$$M_{St} = \pi^{1/2} e^{\phi_4} M_{Pl} \approx 2.1 \times 10^{17} \text{ GeV}, \quad (24)$$

where M_{Pl} is the reduced Planck scale.

It should be kept in mind that values given for the gauge couplings at the string scale are only the *tree-level* results. There are one-loop threshold corrections arising from the $N = 1$ and $N = 2$ open string sectors [45] which may alter these results. In addition, there is exotic matter charged under both observable and hidden sector gauge groups, which are expected to pick up large masses, but could still affect the running of the gauge couplings.

V. CONFINEMENT OF THE HIDDEN SECTOR FIELDS

In addition to the matter content of the MSSM, there is also matter charged under the hidden sector $USp(2)$ gauge groups. These states will generally have fractional electric charges, similar to the so-called ‘cryptons’ [54, 55, 56, 57]. Obviously, no such matter is observed in the low-energy spectrum so these exotic states must receive a large mass. Such a mass may arise if the hidden sector gauge couplings are asymptotically free and become confining at some high energy. Indeed, in the present case we find that the β -functions for the $USp(2)$ groups are all negative [12],

$$\beta_{USp(2)_1} = \beta_{USp(2)_2} = \beta_{USp(2)_3} = \beta_{USp(2)_4} = -3, \quad (25)$$

where we consider all of the chiral exotic particles present even though it is expected that these states will decouple as discussed previously. From the holomorphic gauge kinetic function, the gauge couplings are found to take the values

$$\begin{aligned} g_{USp(2)_1}^2 &= g_{USp(2)_2}^2 \approx 3, \\ g_{USp(2)_3}^2 &= g_{USp(2)_4}^2 \approx 1. \end{aligned} \quad (26)$$

at the string scale. We may then straightforwardly run these couplings to low-energy energy via the one-loop RGE equations,

$$\frac{1}{g^2(\mu)} = \frac{1}{g_{M_{st}}^2} - \frac{1}{8\pi^2} \beta \ln \left(\frac{\mu}{M_{st}} \right), \quad (27)$$

where we find that the couplings for the $USp(2)_1$ and $USp(2)_2$ hidden sector groups will become strong at a scale $\sim 3 \cdot 10^{13}$ GeV, while the couplings for the $USp(2)_3$ and $USp(2)_4$ groups will become strong around $\sim 7 \cdot 10^5$ GeV as shown in Figure 2.

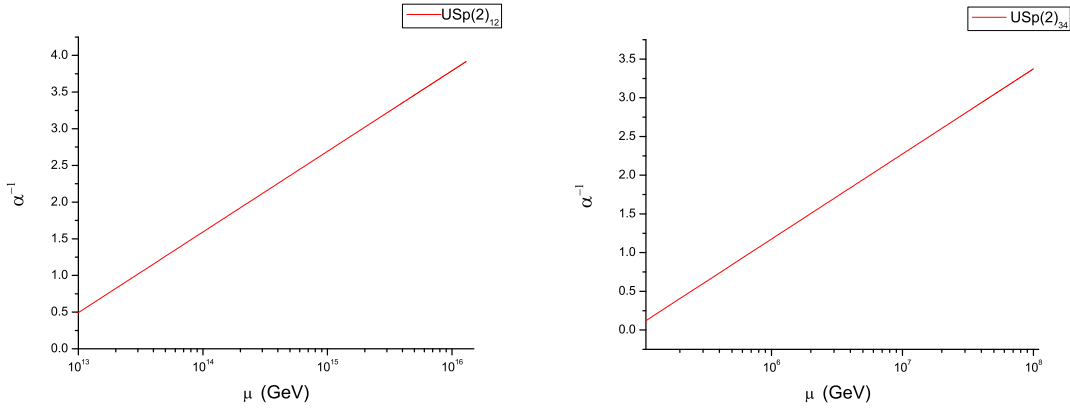


FIG. 2: RGE running of the gauge coupling for $USp(2)_1/USp(2)_2$, $USp(2)_3/USp(2)_4$ hidden sector gauge groups, which become confining at $\approx 3 \cdot 10^{13}$ GeV and $\approx 6 \cdot 10^5$ respectively.

We should note that it is also possible to decouple the chiral exotic states in the manner discussed in section II.

VI. SOFT TERMS AND SUPERPARTNER SPECTRA

Next, we turn to our attention to the soft supersymmetry breaking terms at the GUT scale defined in Eq. (18). In the present analysis, not all the F-terms of the moduli get VEVs for simplicity, as in [58, 59]. As discussed earlier, we will assume that $F_i^t = 0$ so that the soft terms have no dependence on the physical Yukawa couplings. Thus, we consider two cases:

1. The u -moduli dominated SUSY breaking where both the cosmological constant V_0 and the goldstino angle are set to zero, such that $F^s = F^{t^i} = 0$.
2. The u and s -moduli SUSY breaking where the cosmological constant $V_0 = 0$ and $F^s \neq 0$.

A. SUSY breaking with u -moduli dominance

For this case we take $\Theta_s = 0$ so that the F -terms are parameterized by the expression

$$F^{u^i} = \sqrt{3}m_{3/2}(u^i + \bar{u}^i)\Theta_i e^{-i\gamma_i}, \quad (28)$$

where $i = 1, 2, 3$ and with $\sum |\Theta_i|^2 = 1$. With this parametrization, the gaugino mass terms for a stack P may be written as

$$M_P = \frac{-\sqrt{3}m_{3/2}}{\text{Ref}_P} \sum_{j=1}^3 \left(\text{Re} u^j \Theta_j e^{-i\gamma_j} n_P^j m_P^k m_P^l \right) \quad (j, k, l) = (\overline{1}, 2, 3). \quad (29)$$

The Bino mass parameter is a linear combination of the gaugino mass for each stack,

$$M_Y = \frac{1}{f_Y} \sum_P c_P M_P \quad (30)$$

where the coefficients c_P correspond to the linear combination of $U(1)$ factors which define the hypercharge, $U(1)_Y = \sum c_P U(1)_P$.

For the trilinear parameters, we have

$$A_{PQR} = -\sqrt{3}m_{3/2} \sum_{j=1}^3 \left[\Theta_j e^{-i\gamma_j} \left(1 + \left(\sum_{k=1}^3 \xi_{PQ}^{k,j} \Psi(\theta_{PQ}^k) - \frac{1}{4} \right) + \left(\sum_{k=1}^3 \xi_{RP}^{k,j} \Psi(\theta_{RP}^k) - \frac{1}{4} \right) \right) \right] \\ + \frac{\sqrt{3}}{2} m_{3/2} \Theta_3 e^{-i\gamma_1} \quad (31)$$

where P, Q , and R label the stacks of branes whose mutual intersections define the fields present in the corresponding trilinear coupling and the angle differences are defined as

$$\theta_{PQ} = \theta_Q - \theta_P. \quad (32)$$

We must be careful when dealing with cases where the angle difference is negative. Note for the present model, there is always either one or two of the θ_{PQ} which are negative. Let us define the parameter

$$\eta_{PQ} = \text{sgn}(\prod_i \theta_{PQ}^i), \quad (33)$$

such that $\eta_{PQ} = -1$ indicates that only one of the angle differences are negative while $\eta_{PQ} = +1$ indicates that two of the angle differences are negative.

Finally, the squark and slepton (1/4 BPS) scalar mass-squared parameters are given by

$$m_{PQ}^2 = m_{3/2}^2 \left[1 - 3 \sum_{m,n=1}^3 \Theta_m \Theta_n e^{-i(\gamma_m - \gamma_n)} \left(\frac{\delta_{mn}}{4} + \sum_{j=1}^3 (\xi_{PQ}^{j,m\bar{n}} \Psi(\theta_{PQ}^j) + \xi_{PQ}^{j,m} \xi_{PQ}^{j,\bar{n}} \Psi'(\theta_{PQ}^j)) \right) \right] \quad (34)$$

The functions $\Psi(\theta_{PQ}) = \frac{\partial \ln(e^{-\phi_4} \tilde{K}_{PQ})}{\partial \theta_{PQ}}$ in the above formulas defined for $\eta_{PQ} = -1$ are

$$\text{if } \theta_{PQ} < 0 : \quad (35)$$

$$\Psi(\theta_{PQ}^j) = -\gamma_E + \frac{1}{2} \frac{d}{d\theta_{PQ}^j} \ln \Gamma(-\theta_{PQ}^j) - \frac{1}{2} \frac{d}{d\theta_{PQ}^j} \ln \Gamma(1 + \theta_{PQ}^j) + \ln(t^j + \bar{t}^j)$$

$$\text{if } \theta_{PQ} > 0 :$$

$$\Psi(\theta_{PQ}^j) = -\gamma_E + \frac{1}{2} \frac{d}{d\theta_{PQ}^j} \ln \Gamma(1 - \theta_{PQ}^j) - \frac{1}{2} \frac{d}{d\theta_{PQ}^j} \ln \Gamma(\theta_{PQ}^j) + \ln(t^j + \bar{t}^j),$$

and for $\eta_{PQ} = +1$ are

$$\text{if } \theta_{PQ} < 0 : \quad (36)$$

$$\Psi(\theta_{PQ}^j) = \gamma_E + \frac{1}{2} \frac{d}{d\theta_{PQ}^j} \ln \Gamma(1 + \theta_{PQ}^j) - \frac{1}{2} \frac{d}{d\theta_{PQ}^j} \ln \Gamma(-\theta_{PQ}^j) - \ln(t^j + \bar{t}^j)$$

$$\text{if } \theta_{PQ} > 0 : \quad$$

$$\Psi(\theta_{PQ}^j) = \gamma_E + \frac{1}{2} \frac{d}{d\theta_{PQ}^j} \ln \Gamma(\theta_{PQ}^j) - \frac{1}{2} \frac{d}{d\theta_{PQ}^j} \ln \Gamma(1 - \theta_{PQ}^j) - \ln(t^j + \bar{t}^j).$$

The function $\Psi'(\theta_{PQ})$ is just the derivative

$$\Psi'(\theta_{PQ}^j) = \frac{d\Psi(\theta_{PQ}^j)}{d\theta_{PQ}^j}, \quad (37)$$

and $\theta_{PQ}^{j,k}$ and $\theta_{PQ}^{j,k\bar{l}}$ are defined [58] as

$$\xi_{PQ}^{j,k} \equiv (u^k + \bar{u}^k) \frac{\partial \theta_{PQ}^j}{\partial u^k} = \begin{cases} [-\frac{1}{4\pi} \sin(2\pi\theta^j)]_Q^P & \text{when } j = k \\ [\frac{1}{4\pi} \sin(2\pi\theta^j)]_Q^P & \text{when } j \neq k, \end{cases} \quad (38)$$

$$\xi_{PQ}^{j,k\bar{l}} \equiv (u^k + \bar{u}^k)(u^l + \bar{u}^l) \frac{\partial^2 \theta_{PQ}^j}{\partial u^k \partial \bar{u}^l} = \begin{cases} \frac{1}{16\pi} [\sin(4\pi\theta^j) + 4\sin(2\pi\theta^j)]_Q^P & \text{when } j = k = l \\ \frac{1}{16\pi} [\sin(4\pi\theta^j) - 4\sin(2\pi\theta^j)]_Q^P & \text{when } j \neq k = l \\ -\frac{1}{16\pi} [\sin(4\pi\theta^j)]_Q^P & \text{when } j = k \neq l \text{ or } j = l \neq k \\ \frac{1}{16\pi} [\sin(4\pi\theta^j)]_Q^P & \text{when } j \neq k \neq l \neq j. \end{cases} \quad (39)$$

Note that the only explicit dependence of the soft terms on the u and s moduli is in the gaugino mass parameters. The trilinears and scalar mass-squared values depend explicitly only on the angles. However, there is an implicit dependence on the complex structure moduli via the angles made by each D-brane with respect to the orientifold planes.

In contrast to heterotic string models, the gaugino and scalar masses are typically not universal in intersecting D-brane constructions, although in the present case, there is some partial universality of the scalar masses due to the Pati-Salam unification at the string scale. In particular, the trilinear A couplings are found to be equal to a universal parameter, A_0 and the left-handed and right-handed squarks and sleptons respectively are degenerate. The Higgs states arise from the non-chiral sector due to the fact that stacks b , $c1$, and $c2$ are parallel on the third torus. The appropriate Kähler

metric for these states is given by Eq. (12). Thus, the Higgs scalar mass-squared values are found to be

$$m_H^2 = m_{3/2}^2 \left(1 - \frac{3}{2} |\Theta_3|^2 \right). \quad (40)$$

The complex structure moduli u^i , and the four-dimensional dilaton ϕ_4 are fixed by the supersymmetry conditions and gauge coupling unification respectively. The Kähler modulus on the first torus t^1 will be chosen to be consistent with the Yukawa mass matrices calculated in the next section. Thus, the free parameters which remain are $\Theta_{1,2}$, $\text{sgn}(\Theta_3)$, t^2 , t^3 , the phases γ_i , and the gravitino mass $m_{3/2}$. In order to eliminate potential problems with electric dipole moments (EDM's) for the neutron and electron, we set $\gamma_i = 0$. In addition, we set the Kähler moduli on the second and third tori equal to one another, $\text{Re}(t^2) = \text{Re}(t^3) = 0.5$ and take the gravitino mass $m_{3/2} \sim 1$ TeV. Note that the soft terms only have a weak logarithmic dependence on the Kähler moduli.

We constrain the parameter space such that neither the Higgs nor the squark and slepton scalar masses are tachyonic at the high scale, as well as imposing the unitary condition $\Theta_1^2 + \Theta_2^2 + \Theta_3^2 = 1$. In particular, we require $\Theta_3^2 \leq 2/3$, or equivalently $\Theta_1^2 + \Theta_2^2 \geq 1/3$.

To determine the soft terms and superpartner spectra at the low energy scale, we run the RGE's down from the high scale using the code **SuSpect** [60]. In principle, we should be able to determine $\tan \beta$, and the μ and B parameters directly from the model. For the present construction, there is in fact a μ parameter, whose real part corresponds geometrically to the separation between stacks b and c . In the absence of any effects which stabilize the open-string moduli, there are corresponding flat directions in the moduli space. Indeed, the calculation of the Yukawa couplings in the next section will exploit this freedom. Thus, the effective μ -term cannot be calculated until the moduli stabilization issue has been addressed. Essentially the same considerations apply for a determination of $\tan \beta$, which depends upon the explicit values for the neutral component VEV of the Higgs fields, up to an over-all constant. The overall issue of moduli stabilization is discussed in a later section.

For the present work, we will fix these values via the requirement for electroweak symmetry breaking (EWSB), in a similar fashion to [58]. We also choose $\mu > 0$ as favored by $(g - 2)$ and take $\tan \beta$ as a free parameter. We use the value for the top quark mass $m_t = 170.9$ GeV. Then, knowing the low energy spectra, we can then determine the corresponding neutralino relic density. To calculate this, we use the code **MicrOMEGAS** [61]. Some points in the parameter space which give the observed dark matter density are shown in Table IV where we have fixed $\Theta_s = 0$.

TABLE IV: Supersymmetry breaking soft terms at the string scale and resulting neutralino relic density for some specific choices of goldstino angles, with $\Theta_s = 0$.

Θ_1	Θ_2	Θ_3	$M_{\tilde{G}}$ (GeV)	$M_{\tilde{W}}$ (GeV)	$M_{\tilde{B}}$ (GeV)	m_H (GeV)	m_L (GeV)	m_R (GeV)	A_t (GeV)	LSP	Ωh^2
-0.610	0.290	0.737	889	251	422	429	963	466	676	\tilde{B}	0.115
-0.610	0.380	0.695	931	329	416	524	989	478	610	\tilde{B}	0.108
-0.600	0.470	0.647	967	407	411	609	1005	492	531	\tilde{B}	0.113
-0.100	0.870	0.482	1171	753	667	806	684	521	-312	\tilde{B}	0.118
0.0400	0.600	0.799	1211	519	920	205	510	590	-222	\tilde{B}	0.105
0.110	-0.570	0.814	211	-493	564	74	561	631	431	\tilde{B}/\tilde{H}	0.107
0.150	0.660	0.736	1209	571	944	432	529	512	-397	\tilde{B}	0.108
0.010	0.810	0.586	1209	701	793	695	603	510	-371	\tilde{B}	0.094

TABLE V: Low energy supersymmetric particles and their masses (in GeV) for $\Theta_1 = -0.610$, $\Theta_2 = 0.290$, $\Theta_3 = 0.737$, and $\Theta_s = 0$. with $\tan \beta = 46$.

h^0	H^0	A^0	H^\pm	\tilde{g}	χ_1^\pm	χ_2^\pm	χ_1^0	χ_2^0
116.89	826.80	826.81	831.05	1985	192.3	1115.	173.3	192.3
χ_3^0	χ_4^0	\tilde{t}_1	\tilde{t}_2	\tilde{u}_1/\tilde{c}_1	\tilde{u}_2/\tilde{c}_2	\tilde{b}_1	\tilde{b}_2	
-1113.	1114	1477	1789	1949	1761	1638	1791	
\tilde{d}_1/\tilde{s}_1	\tilde{d}_2/\tilde{s}_2	$\tilde{\tau}_1$	$\tilde{\tau}_2$	$\tilde{\nu}_\tau$	$\tilde{e}_1/\tilde{\mu}_1$	$\tilde{e}_2/\tilde{\mu}_2$	$\tilde{\nu}_e/\tilde{\nu}_\mu$	
1950	1760	189.0	928.2	919.5	973.3	488.0	970.1	

A contour plot of the dark matter density is displayed in Fig 3 with $m_{3/2} = 1$ TeV, $\tan \beta = 46$ and for $\Theta_3 > 0$. It can be seen that only small regions of the allowed parameter space can produce the observed dark matter density, which are indicated on the plot as dark bands. Regions which do not satisfy the constraints

$$\Theta_1^2 + \Theta_2^2 + \Theta_3^3 = 1 \quad (41)$$

and

$$\sqrt{\Theta_1^2 + \Theta_2^2} \geq \frac{1}{\sqrt{3}} \quad (42)$$

are indicated on the plots as the light gray shaded areas. The dark gray areas indicate regions of the parameter space where either the neutralino is not the LSP, LEP superpartner mass limits are not satisfied, or for which there is no RGE solution. The viable parameter space may be further

TABLE VI: Low energy supersymmetric particles and their masses (in GeV) for $\Theta_1 = 0.04$, $\Theta_2 = 0.60$, $\Theta_3 = 0.799$, and $\Theta_s = 0$ with $\tan \beta = 46$.

h^0	H^0	A^0	H^\pm	\tilde{g}	χ_1^\pm	χ_2^\pm	χ_1^0	χ_2^0
118.82	1057.1	1057.1	1060.4	2616.	414.6	1478.	390.4	414.6
χ_3^0	χ_4^0	\tilde{t}_1	\tilde{t}_2	\tilde{u}_1/\tilde{c}_1	\tilde{u}_2/\tilde{c}_2	\tilde{b}_1	\tilde{b}_2	
-1475.	1477	1955	2114	2318	2335	2071	2184	
\tilde{d}_1/\tilde{s}_1	\tilde{d}_2/\tilde{s}_2	$\tilde{\tau}_1$	$\tilde{\tau}_2$	$\tilde{\nu}_\tau$	$\tilde{e}_1/\tilde{\mu}_1$	$\tilde{e}_2/\tilde{\mu}_2$	$\tilde{\nu}_e/\tilde{\nu}_\mu$	
2319	2330	474.4	689.6	574.9	620.1	679.0	615.1	

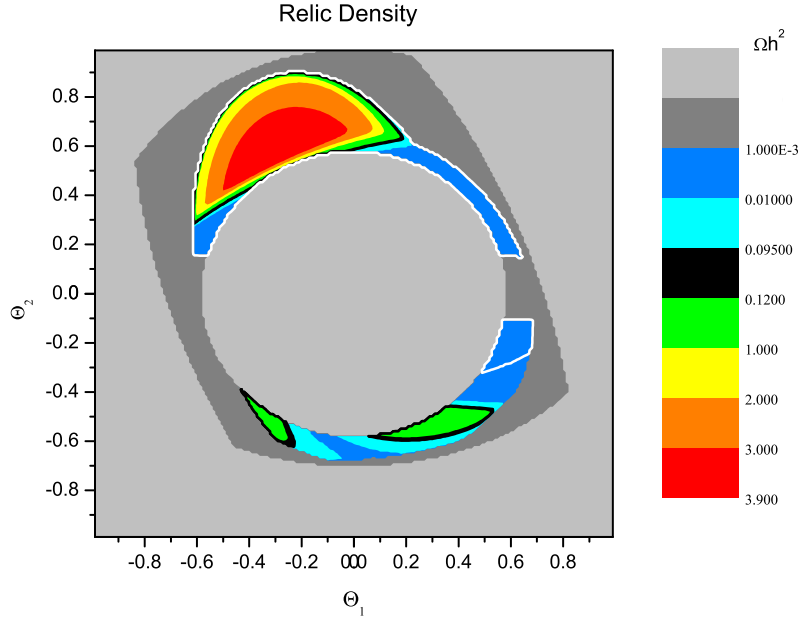


FIG. 3: Contour map of the dark matter density for $\tan \beta = 46$, $\theta_3 > 0$, $\Theta_s = 0$ and $\mu > 0$. The areas in black denote regions where $0.09 \leq \Omega h^2 \leq 0.12$ with a gravitino mass $m_{3/2} = 1$ TeV. The light gray regions are excluded because they do not satisfy the constraints on the soft terms at high scale. The dark grey regions denote regions where either the neutralino is not the LSP, mass limits are not satisfied or for which there is no RGE solution. Regions inside the white contour satisfy the LEP limit, $m_h > 114$ GeV.

constrained by imposing the LEP limit on the lightest CP-even Higgs mass, $m_h \geq 114$ GeV. Regions satisfying this bound are contained within the white contour on the plot. Essentially, this rules out regions of the parameter space with a mixed Bino/Higgsino LSP as the Higgs mass for these regions of the parameter space is always below 114 GeV. A sampling of some of the SUSY

spectra for some of the cases of Table IV are shown in Tables V and VI.

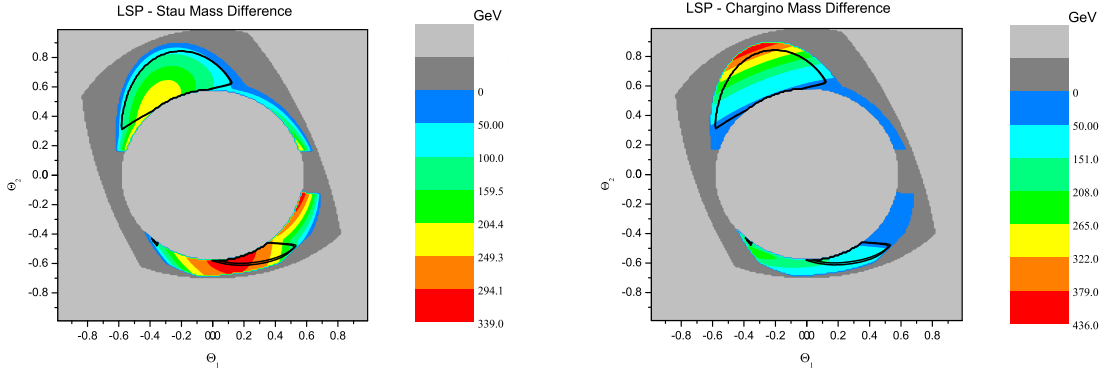


FIG. 4: Contour map of the neutralino-stau mass difference and neutralino-chargino mass difference for $\tan \beta = 46$, $\theta_3 > 0$, $\Theta_s = 0$ and $\mu > 0$. The areas in black denote regions where $0.095 \leq \Omega h^2 \leq 0.125$ with a gravitino mass $m_{3/2} = 1$ TeV. The light gray regions are excluded because they do not satisfy the constraints on the soft terms at high scale. The dark grey regions denote regions where either the neutralino is not the LSP, mass limits are not satisfied or for which there is no RGE solution. The dark matter density within the allowed range coincides with the $\tilde{\chi}_1^0 \tilde{\tau}$ and $\tilde{\chi}_1^0 \tilde{\chi}_1^\pm / \tilde{\chi}_1^0 \tilde{\chi}_2^0$ coannihilation regions where the stau and/or chargino/next-to-lightest neutralino mass is slightly bigger than the lightest neutralino mass.

It can be seen from Fig. 4 that regions of the corresponding parameter space correspond to cases where the lightest neutralino mass is very close to the either or both the lightest chargino/next-to-lightest neutralino $\tilde{\chi}_1^\pm / \tilde{\chi}_2^0$ (which are mass degenerate) and light stau $\tilde{\tau}_1$ mass. In other words, the observed dark matter density is obtained close to the $\tilde{\chi}_1^0 \tilde{\tau}_1$ and/or $\tilde{\chi}_1^0 \tilde{\chi}_1^\pm / \tilde{\chi}_1^0 \tilde{\chi}_2^0$ coannihilation regimes.

The lower bound on the gravitino mass may be estimated for fixed $\tan \beta$ by lowering $m_{3/2}$ until there are no regions of the parameter space for which the Higgs mass satisfies the LEP limit. In this way, it is found that the lower bound satisfies $425 \text{ GeV} \leq m_{3/2} \leq 450 \text{ GeV}$ for $\tan \beta = 46$. This can be seen in Figs. 5, where the region of the parameter space with a Higgs mass above 114 GeV begins to shrink dramatically. For $m_{3/2} = 450 \text{ GeV}$, only very small regions of the viable parameter space results in a Higgs mass above 114 GeV. For $m_{3/2} = 425 \text{ GeV}$, there is no region of the parameter space above this limit. Similar results hold for other values of $\tan \beta$.

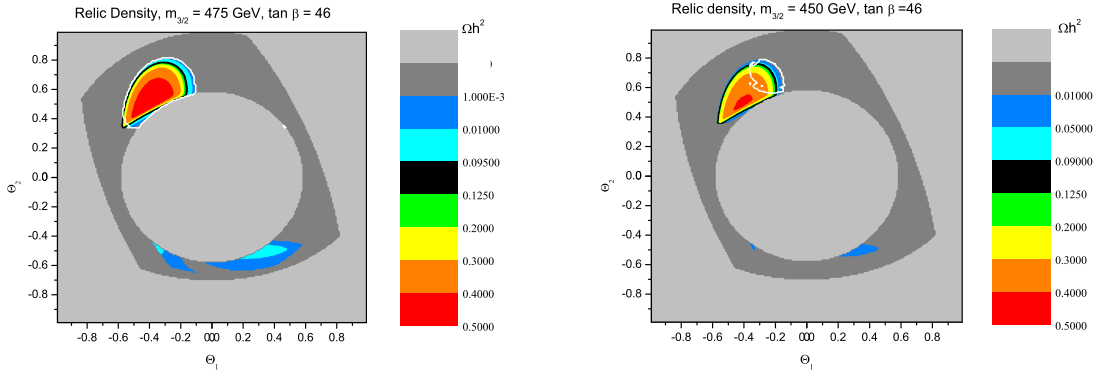


FIG. 5: Contour maps of the relic density for $\tan \beta = 46$, $\theta_3 > 0$, $\Theta_s = 0$ and $\mu > 0$ with a gravitino mass $m_{3/2} = 475$ GeV and $m_{3/2} = 450$ GeV respectively. The areas in black denote regions where $0.09 \leq \Omega h^2 \leq 0.12$. The light gray regions are excluded due to tachyonic scalar masses at the high scale. The dark gray regions denote regions where LEP superpartner mass limits are not satisfied or there is no RGE solution. Regions inside the white contour satisfy the LEP limit, $m_h > 114$ GeV. The viable region of the parameter space is much smaller for $m_{3/2} = 450$ GeV and disappears for $m_{3/2} = 425$ GeV, which constrains the minimum gravitino mass to be in the range $425 \text{ GeV} < m_{3/2} \leq 450 \text{ GeV}$.

B. SUSY breaking via u -moduli and dilaton s

Next, we allow the dilaton s to obtain a non-zero VEV as well as the u -moduli. To do this, we parameterize the F -terms as

$$F^{u^i, s} = \sqrt{3}m_{3/2}[(s + \bar{s})\Theta_s e^{-i\gamma_s} + (u^i + \bar{u}^i)\Theta_i e^{-i\gamma_i}] \quad (43)$$

Clearly, this is a more complicated situation with a much larger set of values over which to scan. The formula for the gaugino mass associated with each stack now becomes

$$M_P = \frac{-\sqrt{3}m_{3/2}}{\text{Ref}_P} \left[\left(\sum_{j=1}^3 \text{Re}(u^j) \Theta_j e^{-i\gamma_j} n_P^j m_P^k m_P^l 2^{-(\beta_k + \beta_l)} \right) + \Theta_s \text{Re}(s) e^{-i\gamma_0} n_P^1 n_P^2 n_P^3 \right], \quad (44)$$

$(j, k, l) = (\overline{1}, 2, 3).$

As before, the Bino mass parameter is a linear combination of the gaugino mass for each stack, and the coefficients corresponding to the linear combination of $U(1)$ factors define the hypercharge.

The trilinear parameters generalize as

$$A_{PQR} = -\sqrt{3}m_{3/2} \sum_{j=0}^3 \left[\Theta_j e^{-i\gamma_j} \left(1 + \left(\sum_{k=1}^3 \xi_{PQ}^{k,j} \Psi(\theta_{PQ}^k) - \frac{1}{4} \right) + \left(\sum_{k=1}^3 \xi_{RP}^{k,j} \Psi(\theta_{RP}^k) - \frac{1}{4} \right) \right) \right] \\ + \frac{\sqrt{3}}{2} m_{3/2} (\Theta_3 e^{-i\gamma_1} + \Theta_s e^{-i\gamma_s}), \quad (45)$$

where Θ_0 corresponds to Θ_s and there is a contribution from the dilaton via the Higgs (1/2 BPS) Kähler metric, which also gives an additional contribution to the Higgs scalar mass-squared values:

$$m_H^2 = m_{3/2}^2 \left[1 - \frac{3}{2} (|\Theta_3|^2 + |\Theta_s|^2) \right]. \quad (46)$$

Finally, the squark and slepton (1/4 BPS) scalar mass-squared parameters are given as before by

$$m_{PQ}^2 = m_{3/2}^2 \left[1 - 3 \sum_{m,n=0}^3 \Theta_m \Theta_n e^{-i(\gamma_m - \gamma_n)} \left(\frac{\delta_{mn}}{4} + \sum_{j=1}^3 (\xi_{PQ}^{j,m\bar{n}} \Psi(\theta_{PQ}^j) + \xi_{PQ}^{j,m} \xi_{PQ}^{j,\bar{n}} \Psi'(\theta_{PQ}^j)) \right) \right] \quad (47)$$

where we now also include the $\Theta_s = \Theta_0$ in the sum. The functions $\Psi(\theta_{PQ})$ and $\Psi'(\theta_{PQ})$ are given as before by Eq. (36) and Eq. (37). The terms associated with the complex moduli in $\xi_{PQ}^{j,k}$ and $\xi_{PQ}^{j,k\bar{l}}$ are the same as those in Eq. (38) and Eq. (39), and the terms associated with the dilaton are given by

$$\xi_{PQ}^{j,s} \equiv (s + \bar{s}) \frac{\partial \theta_{PQ}^j}{\partial s} = \left[-\frac{1}{4\pi} \sin(2\pi\theta^j), \right]_Q^P \quad (48)$$

$$\xi_{PQ}^{j,k\bar{s}} \equiv (u^k + \bar{u}^k)(s + \bar{s}) \frac{\partial^2 \theta_{PQ}^j}{\partial u^k \partial \bar{s}} = \begin{cases} \frac{1}{16\pi} [\sin 4\pi\theta^j]_Q^P & \text{when } j = k \\ -\frac{1}{16\pi} [\sin 4\pi\theta^j]_Q^P & \text{when } j \neq k, \end{cases} \quad (49)$$

and

$$\xi_{PQ}^{j,s\bar{s}} \equiv (s + \bar{s})(s + \bar{s}) \frac{\partial^2 \theta_{PQ}^j}{\partial s \partial \bar{s}} = \frac{1}{16\pi} [\sin 4\pi\theta^j + 4 \sin(2\pi\theta^j)]_Q^P, \quad (50)$$

where $k, l \neq s$. As before, the Θ_i parameters are constrained as $\sum_{i=1}^3 \Theta_i^2 + \Theta_s^2 = 1$. In order to simplify the analysis, we fix Θ_s while varying Θ_3 , Θ_1 , and Θ_2 subject to the unitarity condition. Since there is now another free parameter, the possible parameter space is much larger than in the previous case. Some points in the parameter space which give the observed dark matter density are shown in Table VII where we have fixed $\Theta_s = 0.40$.

We exhibit the relic density as a function of Θ_1 and Θ_2 for the particular case with $\Theta_s = 0.40$ and $\tan \beta = 46$ in Fig 6.

In the figure, only the regions within the white contour satisfy the LEP limit on the Higgs mass. Essentially, this rules out regions of the parameter space with a mixed Bino/Higgsino LSP as the Higgs mass for these regions of the parameter space is always below 114 GeV. A sampling of some of the superpartner spectra for some of the cases of Table VII are shown in Tables VIII, IX, and X below. The viable parameter space is quite large as can be seen from Fig. 7.

TABLE VII: Supersymmetry breaking soft terms at the string scale and resulting neutralino relic density for some specific choices of goldstino angles, with $\Theta_s = 0.40$.

Θ_1	Θ_2	Θ_3	$M_{\tilde{G}}$ (GeV)	$M_{\tilde{W}}$ (GeV)	$M_{\tilde{B}}$ (GeV)	m_H (GeV)	m_L (GeV)	m_R (GeV)	A_t (GeV)	LSP	Ωh^2
-0.490	0.640	0.592	932	207	344	688	832	659	154	\tilde{B}	0.112
-0.450	-0.45	0.771	181	-736	181	327	470	447	842	\tilde{B}/\tilde{H}	0.118
0.140	0.870	0.473	971	407	592	815	470	562	-732	\tilde{B}	0.114
0.380	-0.45	0.808	218	-736	649	142	564	671	-68	\tilde{B}/\tilde{H}	0.105
0.480	-0.41	0.776	220	-701	682	312	692	638	-213	\tilde{B}/\tilde{H}	0.112
0.600	-0.13	0.789	476	-458	856	255	765	520	-516	\tilde{B}	0.112

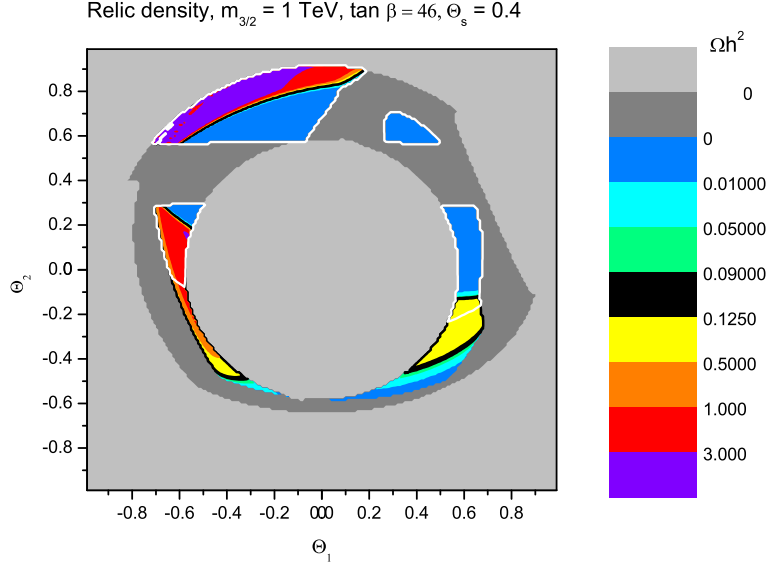


FIG. 6: Contour maps of the relic density for $\tan \beta = 46$, $\theta_s = 0.40 \neq 0$, $\theta_3 = 0.75$, and $\mu > 0$ with a gravitino mass $m_{3/2} = 1$ TeV. The light gray regions are excluded because they do not satisfy the constraints on the soft terms at high scale. Regions inside the white contour satisfy the LEP limit, $m_h > 114$ GeV.

As before, it can be seen that regions of the corresponding parameter space correspond to cases where the the lightest neutralino mass is very close to the either or both the lightest chargino/next-to-lightest neutralino and light stau mass. Thus, the observed dark matter density is obtained close to the $\tilde{\chi}_1^0 \tilde{\tau}_1$ and/or $\tilde{\chi}_1^0 \tilde{\chi}^\pm / \tilde{\chi}_1^0 \tilde{\chi}_2^0$ coannihilation regimes. Similar results hold for other values of $\tan \beta$.

TABLE VIII: Low energy supersymmetric particles and their masses (in GeV) for $\Theta_1 = -0.600$, $\Theta_2 = -0.130$, $\Theta_3 = 0.789$, and $\Theta_s = 0.40$ with $\tan \beta = 46$ and $m_{3/2} = 1$ TeV.

h^0	H^0	A^0	H^\pm	\tilde{g}	χ_1^\pm	χ_2^\pm	χ_1^0	χ_2^0
114.28	600.19	600.2	606.28	1135	390	774.8	-363.2	-390.0
χ_3^0	χ_4^0	\tilde{t}_1	\tilde{t}_2	\tilde{u}_1/\tilde{c}_1	\tilde{u}_2/\tilde{c}_2	\tilde{b}_1	\tilde{b}_2	
769.5	-772.8	856.5	1133.	1253.	1105.	985.4	1126.	
\tilde{d}_1/\tilde{s}_1	\tilde{d}_2/\tilde{s}_2	$\tilde{\tau}_1$	$\tilde{\tau}_2$	$\tilde{\nu}_\tau$	$\tilde{e}_1/\tilde{\mu}_1$	$\tilde{e}_2/\tilde{\mu}_2$	$\tilde{\nu}_e/\tilde{\nu}_\mu$	
1255.	1091.	470.4	796.9	787.6	834.2	607.9	830.5	

TABLE IX: Low energy supersymmetric particles and their masses (in GeV) for $\Theta_1 = -0.490$, $\Theta_2 = 0.640$, $\Theta_3 = 0.592$, and $\Theta_s = 0.40$ with $\tan \beta = 46$ and $m_{3/2} = 1$ TeV.

h^0	H^0	A^0	H^\pm	\tilde{g}	χ_1^\pm	χ_2^\pm	χ_1^0	χ_2^0
117.82	885.60	885.61	889.63	2079	155.1	1110.	139.1	155.1
χ_3^0	χ_4^0	\tilde{t}_1	\tilde{t}_2	\tilde{u}_1/\tilde{c}_1	\tilde{u}_2/\tilde{c}_2	\tilde{b}_1	\tilde{b}_2	
-1107	1109	1573.	1774.	1961.	1900.	1731	1793.	
\tilde{d}_1/\tilde{s}_1	\tilde{d}_2/\tilde{s}_2	$\tilde{\tau}_1$	$\tilde{\tau}_2$	$\tilde{\nu}_\tau$	$\tilde{e}_1/\tilde{\mu}_1$	$\tilde{e}_2/\tilde{\mu}_2$	$\tilde{\nu}_e/\tilde{\nu}_\mu$	
1962.	1900	486.1	793.6	775.9	838.1	669.4	834.5	

VII. YUKAWA COUPLINGS

In addition to the fact that the SM fermions are replicated into three distinct generations, the different generations exhibit an intricate pattern of mass hierarchies. At present, there has been no satisfactory explanation for this. However, in addition to the replication of chirality, intersecting D-brane models may naturally give rise to mass hierarchies and mixing.

The Yukawa couplings in the intersecting D-brane worlds arise from open string world-sheet instantons that connect three D-brane intersections [62]. For a given triplet of intersections, the minimal action world-sheets which contribute to the Yukawa coupling are weighted by a factor $\exp(-A_{abc})$, where A_{abc} is the world-sheet area of the triangles bounded by the branes a, b , and c . Since there are several possible triangles with different areas, mass hierarchies may arise. One may also see that the Yukawa couplings depend on both the D-brane positions in the internal space, as well as on the geometry of the underlying compact manifold. Effectively, these quantities are parameterized by open and closed-string moduli VEVs. Thus, in order to make any definitive predictions for the Yukawa couplings, these moduli must be stabilized.

TABLE X: Low energy supersymmetric particles and their masses (in GeV) for $\Theta_1 = 0.140$, $\Theta_2 = 0.870$, $\Theta_3 = 0.473$, and $\Theta_s = 0.40$ with $\tan \beta = 46$ and $m_{3/2} = 1$ TeV.

h^0	H^0	A^0	H^\pm	\tilde{g}	χ_1^\pm	χ_2^\pm	χ_1^0	χ_2^0
118.02	911.27	911.17	915.16	2136	323.6	1138.	247.4	323.6
χ_3^0	χ_4^0	\tilde{t}_1	\tilde{t}_2	\tilde{u}_1/\tilde{c}_1	\tilde{u}_2/\tilde{c}_2	\tilde{b}_1	\tilde{b}_2	
-1134	1137	1515.	1691.	1911.	1933.	1639	1762.	
\tilde{d}_1/\tilde{s}_1	\tilde{d}_2/\tilde{s}_2	$\tilde{\tau}_1$	$\tilde{\tau}_2$	$\tilde{\nu}_\tau$	$\tilde{e}_1/\tilde{\mu}_1$	$\tilde{e}_2/\tilde{\mu}_2$	$\tilde{\nu}_e/\tilde{\nu}_\mu$	
1912.	1931	267.6	517.4	425.9	540.1	602.7	534.4	

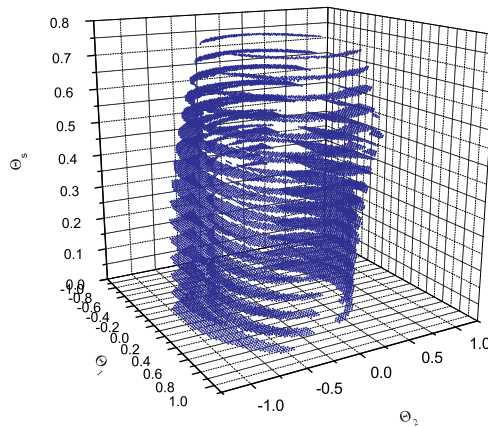


FIG. 7: The viable parameter space with $\Omega h^2 \leq 0.125$ for $\Theta_s \geq 0$.

Despite the promise of intersecting D-brane models in explaining the fermion mass hierarchies and mixings of the Standard Model, they have typically been plagued by a rank-1 problem in the Yukawa mass matrices. This can be traced to the fact that not all of the Standard Model fermions are localized at intersections on the same torus (in the case of toroidal orientifold compactifications). The general flavour structure and selection rules for intersecting D-brane models as been investigated in [63, 64] However, the intersections are all on the first torus for the model of the previous section. Thus the resulting Yukawa mass matrices do not have a rank-1 problem. In the following, we will explore the moduli space of this model in order to see if there are any solutions which may give rise to realistic Yukawa textures, following the analysis of [47], without first addressing the issue of moduli stabilization. Our goal for the present work is simply to see if the observed fermion mass hierarchies may arise in this model and identify the points in the moduli

space where this may happen. We discuss how the moduli might be fixed in a later section.

A. The general form

We start by considering D6 branes in Type IIA, where the D6-branes wrap 3-cycles which intersect at angles on a compact manifold $\mathbf{T}^6 = \mathbf{T}^2 \times \mathbf{T}^2 \times \mathbf{T}^2$. For simplicity, we consider three stacks of D-branes wrapping on a two-torus. The 3-cycles wrapped by the D-branes can be written in a vector form in terms of the wrapping numbers:

$$\begin{aligned} [\Pi_a] &= n_a[a] + m_a[b] : z_a = R(n + Um_a) \cdot x_a, \\ [\Pi_b] &= n_b[a] + m_b[b] : z_b = R(n_b + Um_b) \cdot x_b, \\ [\Pi_c] &= n_c[a] + m_c[b] : z_c = R(n_c + Um_c) \cdot x_c, \end{aligned} \quad (51)$$

where U is the complex structure parameter of the torus and $x \in \mathbf{R}$ arbitrary numbers. The Yukawa coupling involving branes a , b , and c receives a contribution from the areas of the triangles bounded by the triplet of D-branes. To ensure that the triplet of intersections actually form a triangle, we must impose the *closer* condition [47],

$$z_a + z_b + z_c = 0. \quad (52)$$

The wrapping numbers are all integers due to the quantization conditions, so by translating Eq. (52) into the Diophantine equation, the solution is found to be

$$\begin{aligned} x_a &= \frac{I_{bc}}{d}x, \\ x_b &= \frac{I_{ca}}{d}x, \quad x = x_0 + l, \quad x_0 \in \mathbf{R}, \quad l \in \mathbf{Z}, \\ x_c &= \frac{I_{ab}}{d}x, \end{aligned} \quad (53)$$

where I_{ab} is the intersection number, and $d = g.c.d.(I_{ab}, I_{bc}, I_{ca})$ is the greatest common divisor of the intersection numbers. The parameter l indexes the different points in the covering space \mathbf{C} but the same points in the lattice of \mathbf{T}^2 of the triangles. The quantity x_0 is dependent on the different intersection points of two of the D-branes which are indexed by

$$\begin{aligned} i &= 0, 1, \dots, (|I_{ab}| - 1), \\ j &= 0, 1, \dots, (|I_{bc}| - 1), \\ k &= 0, 1, \dots, (|I_{ca}| - 1), \end{aligned} \quad (54)$$

therefore x_0 can be written as

$$x_0(i, j, k) = \frac{i}{I_{ab}} + \frac{j}{I_{ca}} + \frac{k}{I_{bc}}. \quad (55)$$

It is not necessary to require that all branes intersect at the origin. If the position of the stacks is shifted by an amount ϵ_α , $\alpha = a, b, c$, in clockwise directions of stack α by a length in units of $A/||\Pi_\alpha||$ on each torus, then x_0 will be modified as

$$x_0(i, j, k) = \frac{i}{I_{ab}} + \frac{j}{I_{ca}} + \frac{k}{I_{bc}} + \frac{d(I_{ab}\epsilon_c + I_{ca}\epsilon_b + I_{ab}\epsilon_a)}{I_{ab}I_{bc}I_{ca}}. \quad (56)$$

With this parameterization of x_0 , we can now calculate the areas of the triangles, by the area formula of vectors

$$\begin{aligned} A(z_a, z_b) &= \frac{1}{2} \sqrt{|z_a|^2 |z_b|^2 - (\text{Re} z_a \bar{z}_b)^2} \\ \rightarrow A_{ijk}(l) &= \frac{1}{2} (2\pi)^2 A |I_{ab} I_{bc} I_{ca}| \left(\frac{i}{I_{ab}} + \frac{j}{I_{ca}} + \frac{k}{I_{bc}} + \epsilon + l \right)^2, \end{aligned} \quad (57)$$

where ϵ is the total shift effect in Eq. (56),

$$\epsilon = \frac{I_{ab}\epsilon_c + I_{ca}\epsilon_b + I_{bc}\epsilon_a}{I_{ab}I_{bc}I_{ca}} \quad (58)$$

and A is the Kähler structure of the torus, which is generally the area. By adding a real phase $\sigma_{abc} = \text{sign}(I_{ab}I_{bc}I_{ca})$ for the full instanton contribution, the corresponding Yukawa coupling for the three states localized at the intersections indexed by (i, j, k) is [47]

$$Y_{ijk} = h_{qu} \sigma_{abc} \sum_{l \in \mathbf{Z}} \exp\left(-\frac{A_{ijk}(l)}{2\pi\alpha'}\right), \quad (59)$$

where h_{qu} is due to quantum correction as discussed in [48]. The summation can be expressed in terms of a modular theta function for convenient numerical calculation. The real version of this theta function can be written as

$$\vartheta \begin{bmatrix} \delta \\ \phi \end{bmatrix} (t) = \sum_{l \in \mathbf{Z}} e^{-\pi t(\delta+l)^2} e^{2l\pi i(\delta+l)\phi}, \quad (60)$$

so after comparing the parameters, we have

$$\delta = \frac{i}{I_{ab}} + \frac{j}{I_{ca}} + \frac{k}{I_{bc}} + \epsilon, \quad (61)$$

$$\phi = 0, \quad (62)$$

$$t = \frac{A}{\alpha'} |I_{ab} I_{bc} I_{ca}|. \quad (63)$$

a. B-field and Wilson lines

The theta function above is constrained by its real property. However, t can be complex and ϕ can be any number as an overall phase which can be given both a theoretical and phenomenological interpretation.

If we turn on a B-field in the compact space \mathbf{T}^2 , the string will not only couple to the metric but also to this B-field. Then the Kähler structure may be written in a complex form

$$J = B + iA, \quad (64)$$

where the parameter t is replaced by a complex parameter κ

$$\kappa = \frac{J}{\alpha'} |I_{ab} I_{bc} I_{ca}|. \quad (65)$$

We can also include Wilson lines around the compact directions that the D-branes wrap in this construction [47]. To avoid breaking any gauge symmetry, these Wilson lines are chosen up to a phase. If we consider the Yukawa coupling formed by D-branes a , b , and c , wrapping a different one-cycle with Wilson lines in the phases $\exp(2\pi i \theta_a)$, $\exp(2\pi i \theta_b)$, and $\exp(2\pi i \theta_c)$ respectively, then the total phase is a linear combination of each phase weighted by the relative longitude of each segment, determined by the intersection points:

$$e^{2\pi i x_a \theta_a} e^{2\pi i x_b \theta_b} e^{2\pi i x_c \theta_c} = e^{2\pi i x (I_{bc} \theta_a + I_{ca} \theta_b + I_{ab} \theta_c)}. \quad (66)$$

Thus, including these two effects, we obtain a general complex theta function as

$$\vartheta \begin{bmatrix} \delta \\ \phi \end{bmatrix} (\kappa) = \sum_{l \in \mathbf{Z}} e^{\pi i \kappa (\delta + l)^2} e^{2\pi i (\delta + l) \phi}, \quad (67)$$

where

$$\delta = \frac{i}{I_{ab}} + \frac{j}{I_{ca}} + \frac{k}{I_{bc}} + \epsilon, \quad (68)$$

$$\phi = I_{bc} \theta_a + I_{ca} \theta_b + I_{ab} \theta_c, \quad (69)$$

$$\kappa = \frac{J}{\alpha'} |I_{ab} I_{bc} I_{ca}|. \quad (70)$$

b. Other modification

In most of the (semi-)realistic models orientifold planes must be introduced to cancel the RR-tadpoles. As a result, there will be additional fields from the brane images coupling to the

ordinary branes fields as well as themselves. For example, for the triangle formed by branes a , b' , and c , the Yukawa coupling will then depend on the parameters $I_{ab'}$, $I_{b'c}$, and I_{ca} , and the corresponding indicies are i' , j , and k' , where the primed indexes are independent of the unprimed ones.

The other issue is the non-coprime cases. The three intersection numbers are not necessarily coprime, so we have to make sure we do not over-count the repeated parts. The constant d is defined as the *g.c.d.* of the intersection numbers and is introduced in the brane shift parameters. We must then modify the other parameters as well:

$$\phi = \frac{I_{bc}\theta_a + I_{ca}\theta_b + I_{ab}\theta_c}{d}, \quad (71)$$

$$\kappa = \frac{J}{\alpha'} \frac{|I_{ab}I_{bc}I_{ca}|}{d^2}. \quad (72)$$

There is one more constraint which is necessary to ensure non-zero Yukawa couplings: the triangles must be bounded by D-branes. Thus the intersection indexes i , j , and k cannot be arbitrary. They are required to satisfy [47]

$$i + j + k = 0 \pmod{d}. \quad (73)$$

There is one degree of freedom which may ease this constraint, which is an additional parameter in δ : [47]

$$\delta = \frac{i}{I_{ab}} + \frac{j}{I_{ca}} + \frac{k}{I_{bc}} + \epsilon + \frac{s}{d}, \quad (74)$$

where s is a linear combination of i , j , and k , and it is just a shift of counting the triangles since we have required $\{i, j, k\}$ to satisfy (73).

Therefore finally, we can write down a complete form for the Yukawa couplings for D6-branes wrapping on a full compact space $\mathbf{T}^2 \times \mathbf{T}^2 \times \mathbf{T}^2$ as

$$Y_{\{ijk\}} = h_{qu}\sigma_{abc} \prod_{r=1}^3 \vartheta \left[\begin{matrix} \delta^{(r)} \\ \phi^{(r)} \end{matrix} \right] (\kappa^{(r)}), \quad (75)$$

where

$$\vartheta \left[\begin{matrix} \delta^{(r)} \\ \phi^{(r)} \end{matrix} \right] (\kappa^{(r)}) = \sum_{l_r \in \mathbf{Z}} e^{\pi i(\delta^{(r)} + l_r)^2 \kappa^{(r)}} e^{2\pi i(\delta^{(r)} + l_r)\phi^{(r)}}, \quad (76)$$

with $r = 1, 2, 3$ denoting the three two-tori. The input parameters are given by

$$\begin{aligned}\delta^{(r)} &= \frac{i^{(r)}}{I_{ab}^{(r)}} + \frac{j^{(r)}}{I_{ca}^{(r)}} + \frac{k^{(r)}}{I_{bc}^{(r)}} + \frac{d^{(r)}(I_{ab}^{(r)}\epsilon_c^{(r)} + I_{ca}^{(r)}\epsilon_b^{(r)} + I_{ab}^{(r)}\epsilon_a^{(r)})}{I_{ab}I_{bc}I_{ca}} + \frac{s^{(r)}}{d^{(r)}}, \\ \phi^{(r)} &= \frac{I_{bc}^{(r)}\theta_a^{(r)} + I_{ca}^{(r)}\theta_b^{(r)} + I_{ab}^{(r)}\theta_c^{(r)}}{d^{(r)}}, \\ \kappa^{(r)} &= \frac{J^{(r)}}{\alpha'} \frac{|I_{ab}^{(r)}I_{bc}^{(r)}I_{ca}^{(r)}|}{(d^{(r)})^2}.\end{aligned}\tag{77}$$

c. Theta function with characters

It can be complicated to calculate the numerical value of the theta function defined in Eq. (67). Thus, for simplicity the B-field will not be introduced in the following analysis. Then if we define $J' = -iJ = A$ and so $\kappa' = -i\kappa$ for convenience, the theta function turns out to be

$$\begin{aligned}\vartheta \begin{bmatrix} \delta \\ \phi \end{bmatrix} (\kappa') &= \sum_{l \in \mathbf{Z}} e^{-\pi\kappa'(\delta+l)^2} e^{2\pi i(\delta+l)\phi}, \\ \xrightarrow{\text{redefine}} \vartheta \begin{bmatrix} \delta \\ \phi \end{bmatrix} (\kappa) &= e^{-\pi\kappa\delta^2} e^{2\pi i\delta\phi} \vartheta_3(\pi(\phi + i\kappa\delta), e^{-\pi\kappa}),\end{aligned}\tag{78}$$

where ϑ_3 is the Jacobi theta function of the third kind. A plot of the theta function is shown in Fig. 8, with $\phi = 0$.

B. Semi-Realistic Yukawa Textures

(i) Mass Matrices

As mentioned previously, the intersecting D-brane model with matter content shown in Table II has several desirable semi-realistic features, namely three-generations of chiral SM fermions with a minimum of exotic matter, tree-level gauge coupling unification, and the fact that the three intersections required to form the disk diagrams for the Yukawa couplings all occur on the first torus as can be seen from Figure 9. Thus, in our analysis we will focus on the just the first torus, since the contribution from the other two tori will just give an over-all constant. This constant, which is different for the up-type and down-type quark, and charged lepton mass matrices, is unimportant for the present analysis since we will only obtain the mass ratios rather than the absolute fermion masses.

As described in the previous analysis, the Pati-Salam gauge symmetry is broken to the Standard

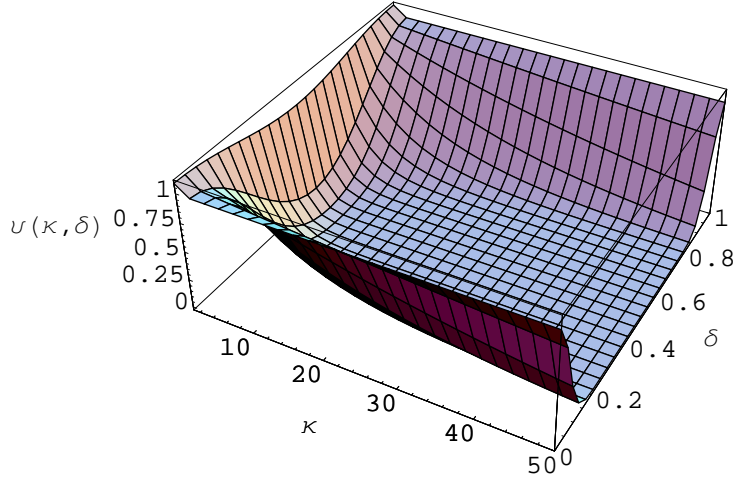


FIG. 8: Theta function as a function of the parameters δ and κ , with $\phi = 0$. The maximum values occur for $\delta = 0$ while the minimum values occur when $\delta = 1/2$.

Model by a process which involves brane-splitting,

$$a \rightarrow a_1 + a_2, \quad c \rightarrow c_1 + c_2. \quad (79)$$

so that the Standard Model quarks and leptons arise from

$$\begin{aligned} F_L(Q_L, L_L) &\rightarrow Q_L + L \\ F_R(Q_R, L_R) &\rightarrow U_R + D_R + E_R + N. \end{aligned} \quad (80)$$

The Yukawa couplings for the quarks and leptons are then given by the superpotential

$$W_Y = Y_{ijk}^U Q_L^i U_R^j H_U^k + Y_{ijk}^D Q_L^i D_R^j H_D^k + Y_{ijk}^L L^i E^j H_D^k, \quad (81)$$

where it should be kept in mind that there are six vector pairs of Higgs multiplets, each of which may receive a VEV.

For the model under consideration, the intersection numbers on each torus are given by

$$\begin{aligned} I_{ab}^{(1)} &= 3, \quad I_{ab}^{(2)} = -1, \quad I_{ab}^{(3)} = -1, \\ I_{ca}^{(1)} &= -3, \quad I_{ca}^{(2)} = -1, \quad I_{ca}^{(3)} = 1, \\ I_{bc}^{(1)} &= -6, \quad I_{bc}^{(2)} = 1, \quad I_{bc}^{(3)} = 0. \end{aligned}$$

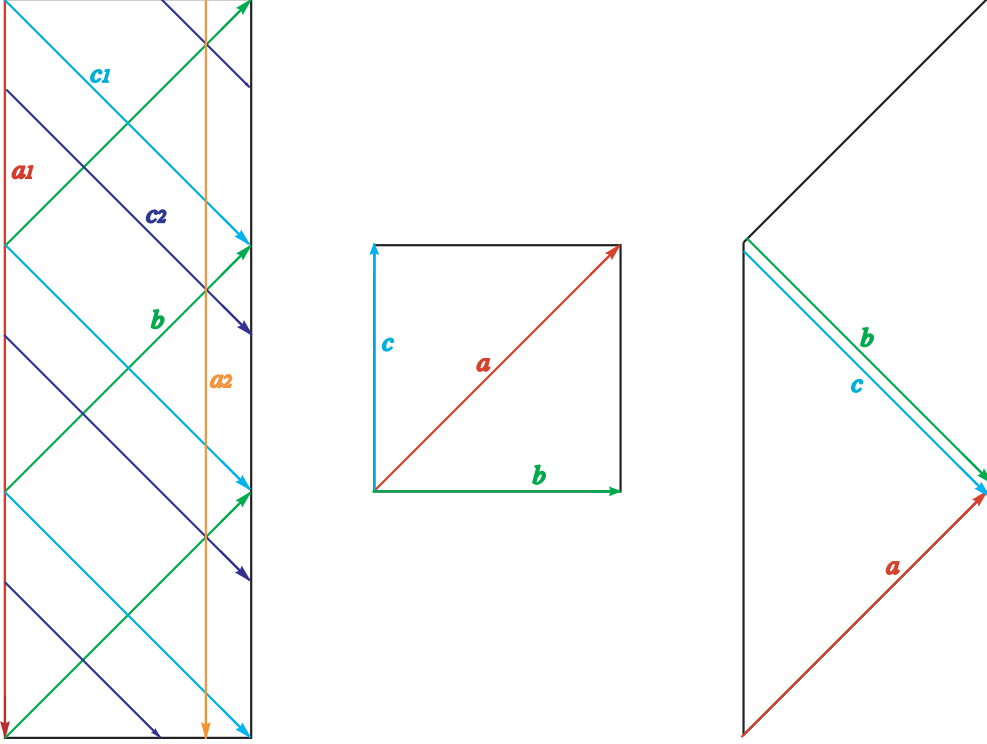


FIG. 9: Brane configuration for the three two-tori. The SM fermion mass hierarchies primarily result from the intersections on the first torus.

These intersection numbers are not coprime, so that we need to have $d^{(1)} = g.c.d.(I_{ab}^{(1)}, I_{bc}^{(1)}, I_{ca}^{(1)}) = 3$, $d^{(2)} = 1$. Note that we do not need $d^{(3)}$ since the intersections do not form any triangles on the

third torus. Thus the parameters of the theta functions defined in Eq. 77 are given by

$$\begin{aligned}\delta^{(1)} &= \frac{i^{(1)}}{3} - \frac{j^{(1)}}{3} - \frac{k^{(1)}}{6} + \frac{\epsilon_c^{(1)} - \epsilon_b^{(1)} - 2\epsilon_a^{(1)}}{6} + \frac{s^{(1)}}{3}, \\ \delta^{(2)} &= -\epsilon_c^{(2)} - \epsilon_b^{(2)} + \epsilon_a^{(2)}, \\ \delta^{(3)} &= -\epsilon_c^{(3)} + \epsilon_b^{(3)},\end{aligned}\tag{82}$$

$$\begin{aligned}\phi^{(1)} &= \theta_c^{(1)} - \theta_b^{(1)} - 2\theta_a^{(1)}, \\ \phi^{(2)} &= -\theta_c^{(2)} - \theta_b^{(2)} + \theta_a^{(2)}, \\ \phi^{(3)} &= -\theta_c^{(3)} + \theta_b^{(3)},\end{aligned}\tag{83}$$

$$\begin{aligned}\kappa^{(1)} &= \frac{6J^{(1)}}{\alpha'}, \\ \kappa^{(2)} &= \frac{J^{(2)}}{\alpha'}, \\ \kappa^{(3)} &= 0,\end{aligned}\tag{84}$$

where $i = 0 \dots 2$, $j = 0 \dots 2$, and $k = 0 \dots 5$, indexing the left-handed fermions, right-handed fermions, and Higgs fields respectively. For mathematical convenience we redefine the shift on each torus as

$$\begin{aligned}\epsilon^{(1)} &\equiv \frac{\epsilon_c^{(1)} - \epsilon_b^{(1)} - 2\epsilon_a^{(1)}}{6}, \\ \epsilon^{(2)} &\equiv -\epsilon_c^{(2)} - \epsilon_b^{(2)} + \epsilon_a^{(2)}, \\ \epsilon^{(3)} &\equiv -\epsilon_c^{(3)} + \epsilon_b^{(3)}.\end{aligned}\tag{85}$$

The intersection numbers on the second and third tori are either one or zero, so their contribution to the Yukawa couplings will be an over-all constant. For a given triplet of intersections to be connected by an instanton, the selection rule

$$i^{(1)} + j^{(1)} + k^{(1)} = 0 \bmod 3\tag{86}$$

should be satisfied. Then, the Yukawa coupling matrices will take the following form:

$$\begin{aligned}
Y_{k=0}^{(1)} &\sim \begin{pmatrix} a_{000} & 0 & 0 \\ 0 & 0 & a_{120} \\ 0 & a_{210} & 0 \end{pmatrix}, \quad Y_{k=1}^{(1)} \sim \begin{pmatrix} 0 & 0 & a_{021} \\ 0 & a_{111} & 0 \\ a_{201} & 0 & 0 \end{pmatrix}, \quad Y_{k=2}^{(1)} \sim \begin{pmatrix} 0 & a_{012} & 0 \\ a_{102} & 0 & 0 \\ 0 & 0 & a_{222} \end{pmatrix}, \\
Y_{k=3}^{(1)} &\sim \begin{pmatrix} a_{003} & 0 & 0 \\ 0 & 0 & a_{123} \\ 0 & a_{213} & 0 \end{pmatrix}, \quad Y_{k=4}^{(1)} \sim \begin{pmatrix} 0 & 0 & a_{024} \\ 0 & a_{114} & 0 \\ a_{204} & 0 & 0 \end{pmatrix}, \quad Y_{k=5}^{(1)} \sim \begin{pmatrix} 0 & a_{015} & 0 \\ a_{105} & 0 & 0 \\ 0 & 0 & a_{225} \end{pmatrix}.
\end{aligned} \tag{87}$$

By choosing a different linear function for $s^{(1)}$, some independent modes with non-zero eigenvalues are available, which are listed below.

(i) $s^{(1)} = 0$

$$\begin{aligned}
a_{000} = a_{102} = a_{204} &= \vartheta \begin{bmatrix} \epsilon^{(1)} \\ \phi^{(1)} \end{bmatrix} \left(\frac{6J^{(1)}}{\alpha'} \right) \equiv A, \\
a_{210} = a_{012} = a_{114} &= \vartheta \begin{bmatrix} \epsilon^{(1)} + \frac{1}{3} \\ \phi^{(1)} \end{bmatrix} \left(\frac{6J^{(1)}}{\alpha'} \right) \equiv B, \\
a_{120} = a_{222} = a_{024} &= \vartheta \begin{bmatrix} \epsilon^{(1)} - \frac{1}{3} \\ \phi^{(1)} \end{bmatrix} \left(\frac{6J^{(1)}}{\alpha'} \right) \equiv C, \\
a_{021} = a_{123} = a_{225} &= \vartheta \begin{bmatrix} \epsilon^{(1)} + \frac{1}{6} \\ \phi^{(1)} \end{bmatrix} \left(\frac{6J^{(1)}}{\alpha'} \right) \equiv D, \\
a_{201} = a_{003} = a_{105} &= \vartheta \begin{bmatrix} \epsilon^{(1)} + \frac{1}{2} \\ \phi^{(1)} \end{bmatrix} \left(\frac{6J^{(1)}}{\alpha'} \right) \equiv E, \\
a_{111} = a_{213} = a_{015} &= \vartheta \begin{bmatrix} \epsilon^{(1)} - \frac{1}{6} \\ \phi^{(1)} \end{bmatrix} \left(\frac{6J^{(1)}}{\alpha'} \right) \equiv F,
\end{aligned} \tag{88}$$

in other words

$$\begin{aligned}
Y_{k=0}^{(1)} &\sim \begin{pmatrix} A & 0 & 0 \\ 0 & 0 & C \\ 0 & B & 0 \end{pmatrix}, \quad Y_{k=1}^{(1)} \sim \begin{pmatrix} 0 & 0 & D \\ 0 & F & 0 \\ E & 0 & 0 \end{pmatrix}, \quad Y_{k=2}^{(1)} \sim \begin{pmatrix} 0 & B & 0 \\ A & 0 & 0 \\ 0 & 0 & C \end{pmatrix}, \\
Y_{k=3}^{(1)} &\sim \begin{pmatrix} E & 0 & 0 \\ 0 & 0 & D \\ 0 & F & 0 \end{pmatrix}, \quad Y_{k=4}^{(1)} \sim \begin{pmatrix} 0 & 0 & C \\ 0 & B & 0 \\ A & 0 & 0 \end{pmatrix}, \quad Y_{k=5}^{(1)} \sim \begin{pmatrix} 0 & F & 0 \\ E & 0 & 0 \\ 0 & 0 & D \end{pmatrix}.
\end{aligned} \tag{89}$$

(ii) $s^{(1)} = j$

$$\begin{aligned}
Y_{k=0}^{(1)} &\sim \begin{pmatrix} A & 0 & 0 \\ 0 & 0 & B \\ 0 & C & 0 \end{pmatrix}, \quad Y_{k=1}^{(1)} \sim \begin{pmatrix} 0 & 0 & F \\ 0 & D & 0 \\ E & 0 & 0 \end{pmatrix}, \quad Y_{k=2}^{(1)} \sim \begin{pmatrix} 0 & C & 0 \\ B & 0 & 0 \\ 0 & 0 & A \end{pmatrix}, \\
Y_{k=3}^{(1)} &\sim \begin{pmatrix} E & 0 & 0 \\ 0 & 0 & F \\ 0 & D & 0 \end{pmatrix}, \quad Y_{k=4}^{(1)} \sim \begin{pmatrix} 0 & 0 & B \\ 0 & C & 0 \\ A & 0 & 0 \end{pmatrix}, \quad Y_{k=5}^{(1)} \sim \begin{pmatrix} 0 & D & 0 \\ F & 0 & 0 \\ 0 & 0 & E \end{pmatrix}.
\end{aligned} \tag{90}$$

(iii) $s^{(1)} = -i$

$$\begin{aligned}
Y_{k=0}^{(1)} &\sim \begin{pmatrix} A & 0 & 0 \\ 0 & 0 & B \\ 0 & C & 0 \end{pmatrix}, \quad Y_{k=1}^{(1)} \sim \begin{pmatrix} 0 & 0 & D \\ 0 & E & 0 \\ F & 0 & 0 \end{pmatrix}, \quad Y_{k=2}^{(1)} \sim \begin{pmatrix} 0 & B & 0 \\ C & 0 & 0 \\ 0 & 0 & A \end{pmatrix}, \\
Y_{k=3}^{(1)} &\sim \begin{pmatrix} E & 0 & 0 \\ 0 & 0 & F \\ 0 & D & 0 \end{pmatrix}, \quad Y_{k=4}^{(1)} \sim \begin{pmatrix} 0 & 0 & C \\ 0 & A & 0 \\ B & 0 & 0 \end{pmatrix}, \quad Y_{k=5}^{(1)} \sim \begin{pmatrix} 0 & F & 0 \\ D & 0 & 0 \\ 0 & 0 & E \end{pmatrix}.
\end{aligned} \tag{91}$$

The cases $s^{(1)} = k/2$ and $s^{(1)} = 2j$ are not considered since there they may forbid three different real eigenvalues. We will take case (iii) for the following discussion.

The most general form for a given mass matrix can then be given as

$$\mathcal{M} \sim \begin{pmatrix} Av_1 + Ev_4 & Bv_3 + Fv_6 & Dv_2 + Cv_5 \\ Cv_3 + Dv_6 & Av_5 + Ev_2 & Bv_1 + Fv_4 \\ Fv_2 + Bv_5 & Cv_1 + Dv_4 & Av_3 + Ev_6 \end{pmatrix}, \tag{92}$$

where $v_i = \langle H_i \rangle$ are the different VEVs of the six Higgs fields present in the model.

$$(M_u)_{ij} \sim \begin{pmatrix} A^U H_u^1 + E^U H_u^4 & B^U H_u^3 + F^U H_u^6 & D^U H_u^2 + C^U H_u^5 \\ C^U H_u^3 + D^U H_u^6 & A^U H_u^5 + E^U H_u^2 & B^U H_u^1 + F^U H_u^4 \\ F^U H_u^2 + B^U H_u^5 & C^U H_u^1 + D^U H_u^4 & A^U H_u^3 + E^U H_u^6 \end{pmatrix}, \tag{93}$$

$$(M_d)_{ij} \sim \begin{pmatrix} A^D H_d^1 + E^D H_d^4 & B^D H_d^3 + F^D H_d^6 & D^D H_d^2 + C^D H_d^5 \\ C^D H_d^3 + D^D H_d^6 & A^D H_d^5 + E^D H_d^2 & B^D H_d^1 + F^D H_d^4 \\ F^D H_d^2 + B^D H_d^5 & C^D H_d^1 + D^D H_d^4 & A^D H_d^3 + E^D H_d^6 \end{pmatrix}, \tag{94}$$

$$(M_l)_{ij} \sim \begin{pmatrix} A^E H_d^1 + E^E H_d^4 & B^E H_d^3 + F^E H_d^6 & D^E H_d^2 + C^E H_d^5 \\ C^E H_d^3 + D^E H_d^6 & A^E H_d^5 + E^E H_d^2 & B^E H_d^1 + F^E H_d^4 \\ F^E H_d^2 + B^E H_d^5 & C^E H_d^1 + D^E H_d^4 & A^E H_d^3 + E^E H_d^6 \end{pmatrix}. \quad (95)$$

The two light Higgs mass eigenstates which arise by fine-tuning the superpotential shown in Eq. 4 would then be different linear combinations of the six Higgs fields present in the model. For a given set of VEVs for the Higgs fields chosen to obtain the desired Yukawa matrices, we can then write the light Higgs eigenstates as

$$H_{u,d} = \sum \frac{v_{u,d}^i}{\sqrt{\sum (v_{u,d}^i)^2}} H_{u,d}^i, \quad (96)$$

with $v_{u,d}^i = \langle H_{u,d}^i \rangle$.

One may see from the form of the above mass matrices that there is a natural mass hierarchy among the up-quarks, down-quarks and leptons which has a geometric interpretation related to the position of the different D-branes, as parameterized by the shifts ϵ_i . Recall that the Pati-Salam gauge symmetry has been broken to the SM by a process which involves splitting the stacks of D-branes as shown in Fig. 1. The left-handed quarks are localized at the intersections between stacks $a1$ and b , the right-handed up-type quarks are localized between stacks $a1$ and $c1$, while the right-handed down-type quarks are localized between stacks $a1$ and $c2$. Thus, if stack $c2$ is shifted on the torus by an amount ϵ_{c2} while stack $c1$ is unshifted ($\epsilon_{c1} = 0$), then the down-type quark masses are naturally suppressed relative to the up-type quarks. Similarly, the left-handed charged leptons are localized at the intersection between stack $a2$ and b , while the right-handed charged leptons are localized at the intersection between stacks $a2$ and $c2$. Since stack $a2$ will be shifted by some amount ϵ_{a2} , the resulting charged lepton masses will be naturally suppressed relative to the down-type quarks. Thus, from purely geometric considerations, we expect

$$m_u > m_d > m_l. \quad (97)$$

It is also clear from the form of the mass matrices that the mass hierarchies between the different up-type quarks among themselves, the different down-type quarks among themselves, and the different charged leptons among themselves are due primarily to the different Higgs neutral component VEVs. Effectively, these values will be determined by fine-tuning the superpotential so that there are only two Higgs eigenstates as shown in Eq. 96. Ideally, one would like to be able to dynamically determine the Higgs eigenstates from first principles rather than fine-tuning the superpotential. However, it does not seem possible to do this at least until the issue of moduli stabilization has been fully addressed.

If we define D_u and D_d as the mass diagonal matrices of up and down-type quarks respectively,

$$U_L^u M_u U_R^{u\dagger} = D_u, \quad U_L^d M_d U_R^{d\dagger} = D_d, \quad V_{CKM} = U_L^u U_L^{d\dagger}, \quad (98)$$

where U^i are unitary matrices, then the squared mass matrices are $M_u M_u^\dagger$ and $M_d M_d^\dagger$. In the Standard Model, we can always make quark mass matrices M_u and M_d Hermitian by suitable transformation of the right-handed fields. If we take a case that the M_d is very close to the diagonal matrix for down-type quark, in other words, U_L^d and U_R^d are very close to the unit matrix with very small off-diagonal terms, then

$$V_{CKM} \simeq U^u U^{d\dagger} \simeq U^u, \quad (99)$$

where we have transformed away the right-handed effects and make them the same as the left-handed ones. Then the mass matrix of the up-type quarks is

$$M_u \sim V_{CKM}^\dagger D_u V_{CKM}. \quad (100)$$

(ii) An Example

For different superpartner spectra, we may determine the mass matrices for quarks and leptons by running the RGE's up to the unification scale. For example, for $\tan\beta \approx 50$ the CKM matrix at the unification scale $\mu = M_X$ may be determined to be [65, 66]

$$V_{CKM} = \begin{pmatrix} 0.9754 & 0.2205 & -0.0026i \\ -0.2203e^{0.003^\circ i} & 0.9749 & 0.0318 \\ 0.0075e^{-19^\circ i} & -0.0311e^{1.0^\circ i} & 0.9995 \end{pmatrix}, \quad (101)$$

and the diagonal quark mass matrices D_u and D_d may be written

$$D_u = m_t \begin{pmatrix} 0.0000139 & 0 & 0 \\ 0 & 0.00404 & 0 \\ 0 & 0 & 1 \end{pmatrix}, \quad D_d = m_b \begin{pmatrix} 0.00141 & 0 & 0 \\ 0 & 0.0280 & 0 \\ 0 & 0 & 1 \end{pmatrix}. \quad (102)$$

Then the absolute value of M_u turns out to be

$$|M_u| = m_t \begin{pmatrix} 0.000266 & 0.00109 & 0.00747 \\ 0.00109 & 0.00481 & 0.0310 \\ 0.00747 & 0.0310 & 0.999 \end{pmatrix}. \quad (103)$$

We can then fine-tune the parameters and Higgs VEVs in Eqs. (93), (94), and (95) to fit these mass matrices. It looks at the first glance that the solution can be easily found, but we should

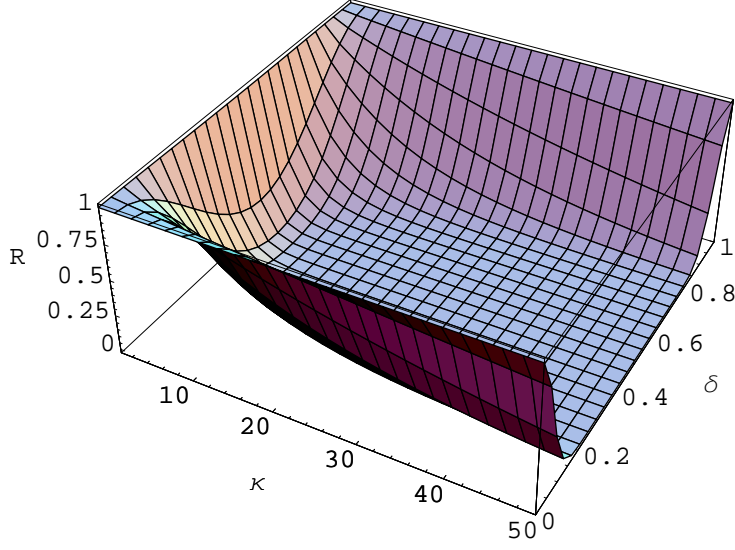


FIG. 10: Ratio of theta functions $R = [e^{-\pi\kappa\delta^2}\vartheta_3(i\pi\kappa\delta, e^{-\pi\kappa})]/[\vartheta_3(0, e^{-\pi\kappa})]$.

keep in mind that the six parameters from the theta function controlled by the D-brane shifts and Wilson-line phases are *not* independent. In doing so, we are essentially constrained by the off-diagonal terms, as can be seen by comparing Eq. 93 with Eq. 103. For example, the (11) element of $|M_u|$ is 0.00109, while the corresponding element of the fitted mass matrix is $Bv_3 + Fv_6$. However, the diagonal (33) element of the fitted matrix is given by $Av_3 + Ev_6$ which should be of order unity. Thus, to fit the mass matrix we must require

$$\frac{Bv_3 + Fv_6}{Av_3 + Ev_6} \approx 0.00109, \quad (104)$$

which effectively means that $\frac{B}{A} \ll 1$ and $\frac{F}{E} \ll 1$.

In Fig. 10, we plot the ratio

$$\frac{\vartheta \begin{bmatrix} \delta \\ 0 \end{bmatrix}(\kappa) = e^{-\pi\kappa\delta^2} \vartheta_3(i\pi\kappa\delta, e^{-\pi\kappa})}{\vartheta \begin{bmatrix} \delta=0 \\ 0 \end{bmatrix}(\kappa) = \vartheta_3(0, e^{-\pi\kappa})}. \quad (105)$$

It can be seen from this plot that the off-diagonal terms will be naturally suppressed relative to the diagonal elements. In order to satisfy the conditions shown in Eq. 104 to fit the up-type quark mass matrix, must must allow κ to be large enough such that $e^{-\pi\kappa} \approx 0$. This in effect means that

$\vartheta_3(i\pi\kappa\delta, e^{-\pi\kappa}) = 1$, so that

$$\begin{aligned} A &= e^{-\pi\kappa\epsilon^2}, & B &= e^{-\pi\kappa(\epsilon+1/3)^2}, & C &= e^{-\pi\kappa(\epsilon-1/3)^2}, \\ D &= e^{-\pi\kappa(\epsilon+1/6)^2}, & E &= e^{-\pi\kappa(\epsilon+1/2)^2}, & F &= e^{-\pi\kappa(\epsilon-1/6)^2}. \end{aligned} \quad (106)$$

On comparing M_u and Eq. (93) we can obtain a set of parameters which will give the desired solution. For example, if we set $\frac{6J^{(1)}}{\alpha'} = \kappa = 39.6$ and $\epsilon^{(1)U} = 0$, where $\epsilon_a^{(1)U} = \epsilon_{a^1}^{(1)} = 0$, $\epsilon_b^{(1)U} = \epsilon_b^{(1)} = 0$, and $\epsilon_c^{(1)U} = \epsilon_{c^1}^{(1)} = 0$, then

$$\begin{aligned} A^U &= 1, & v_u^1 &= 0.000266, \\ B^U &= 0.000001, & v_u^2 &= 0.236, \\ C^U &= 0.000001, & v_u^3 &= 0.999, \\ D^U &= 0.0316, & v_u^4 &= 0.981, \\ E^U &= 0.0, & v_u^5 &= 0.00481, \\ F^U &= 0.0316, & v_u^6 &= 0.0345, \end{aligned} \quad (107)$$

which may reproduce exactly the mass matrix Eq. 103.

Similarly, after fixing the Kähler modulus from what is needed to obtain the correct off-diagonal terms for the up-type quark mass matrix, we can then obtain a result for M_d . For the present case, we have $\frac{m_\tau}{m_b} = 1.58$ which is obtained from the previous analysis of the soft-terms for a point in the parameter space satisfying all constraints. With the choices $\epsilon^{(1)D} = 0.061$, where $\epsilon_a^{(1)D} = \epsilon_{a^1}^{(1)} = 0$, $\epsilon_b^{(1)D} = \epsilon_b^{(1)} = 0$, and $\epsilon_c^{(1)D} = \epsilon_{c^2}^{(1)} = 0.366$ (by Eq. (85)), the desired solution may be obtained with

$$\begin{aligned} A^D &= 0.629, & v_d^1 &= 0.00224, \\ B^D &= 0.0, & v_d^2 &= 0.0, \\ C^D &= 0.000098, & v_d^3 &= 1.58, \\ D^D &= 0.00158, & v_d^4 &= 0.0, \\ E^D &= 0.0, & v_d^5 &= 0.0445, \\ F^D &= 0.249, & v_d^6 &= 0.0001, \end{aligned} \quad (108)$$

The calculated mass matrix M_d is thus given as

$$|M_d| \sim m_b \begin{pmatrix} 0.00141 & 0.000025 & 0.000004 \\ 0.000155 & 0.0280 & 0.0 \\ 0.0 & 0.000000220 & 1 \end{pmatrix} \sim D_d. \quad (109)$$

Note that the down-type quark mass matrix and the lepton mass matrix both involve the same Higgs fields. Thus, once the parameters needed to fit the down-type mass matrix are fixed, the

only freedom in calculating the lepton mass matrix is from the geometric position of each brane. To fit the lepton matrix consistent with the down-type quark matrix, we may choose $\epsilon^{(1)L} = 0.0$, where $\epsilon_a^{(1)L} = \epsilon_{a^2}^{(1)} = 0.183$, $\epsilon_b^{(1)L} = \epsilon_b^{(1)} = 0.0$, $\epsilon_c^{(1)L} = \epsilon_{c^2}^{(1)} = 0.366$, then

$$\begin{aligned} A^L &= 1.0, & B^L &= 0.000001, \\ C^L &= 0.000001, & D^L &= 0.0316, \\ E^L &= 0.0, & F^L &= 0.0316, \end{aligned} \tag{110}$$

so that the fitted mass matrix of leptons is given as

$$|M_l| \sim m_b \begin{pmatrix} 0.00224 & 4.74 \times 10^{-6} & 4.45 \times 10^{-8} \\ 4.74 \times 10^{-6} & 0.0445 & 2.24 \times 10^{-9} \\ 4.45 \times 10^{-8} & 2.24 \times 10^{-9} & 1.58 \end{pmatrix} \tag{111}$$

$$= m_\tau \begin{pmatrix} 0.00142 & 3.0 \times 10^{-6} & 2.82 \times 10^{-8} \\ 3.0 \times 10^{-6} & 0.0282 & 1.42 \times 10^{-9} \\ 2.82 \times 10^{-8} & 1.42 \times 10^{-9} & 1.0 \end{pmatrix}. \tag{112}$$

We may compare the eigenvalues $m_\tau\{0.014, 0.028, 1\}$ for the fitted matrix with the extrapolated lepton masses obtained from running the RGEs up to the GUT scale:

$$D_l = m_\tau \begin{pmatrix} 0.000217 & 0 & 0 \\ 0 & 0.0458 & 0 \\ 0 & 0 & 1 \end{pmatrix}. \tag{113}$$

Thus, the electron mass comes out to be too big by a factor of six, while the muon mass is 60% too small. However, the tau lepton mass does come out correctly. This result can be understood by considering that the only difference between the down-type quark and lepton mass matrices is an overall exponential factor which results from the additional shift for the leptonic brane, ϵ_{a1} . Although this result seems to give the wrong answers for the electron and muon masses, it should be kept in mind that these are only tree-level results. Indeed, it is of interest that the error in the obtained lepton masses seems to increase with decreasing mass. There could indeed be other corrections, such as those coming from higher-dimensional operators, which would contribute most greatly to the electron and muon masses since they are quite small.

In short, the above mass matrices can produce the correct quark masses and CKM mixings, and the correct τ lepton mass at the electroweak scale. The electron mass is about $5 \sim 6.5$ times larger than the expected value, while the muon mass is about $50 \sim 60\%$ too small. Similar to GUTs, we end up with roughly the wrong fermion mass relation $m_e/m_\mu \cong m_d/m_s$. The correct electron

and muon masses may in principle be generated via high-dimensional operators by introducing the vector-like Higgs fields from the ac' sector [67]. Moreover, the suitable neutrino masses and mixings can be generated via the seesaw mechanism by choosing suitable Majorana mass matrix for the right-handed neutrinos.

VIII. A COMMENT ON MODULI STABILIZATION

In the previous section, it has been demonstrated that it is possible to obtain Yukawa textures which can reproduce the observed fermion mass hierarchies and mixings (extrapolated at the unification scale). Although this is a very interesting result, it is clear from this analysis that the Yukawa couplings depend on several parameters which are not determined within the model. Rather, random values for these parameters have been chosen by hand in order to fit the experimental results. Thus, it is far from clear that this model in its current form can offer a completely satisfactory explanation for the observed fermion mass hierarchies and mixings.

Given a concrete string model, the low-energy observables such as particle couplings and resulting masses are functions of the open and closed string moduli. In particular, we can see from the analysis of the previous section that the Yukawa couplings depend on the position of each stack of branes on the tori as well as on the Kähler moduli. Thus, if these moduli can be fixed dynamically, then the possible Yukawa mass textures would be tightly constrained. Indeed, once these moduli are fixed, the only remaining freedom is in the Higgs sector, namely the specific linear combination of the six pairs of Higgs states which must be fine-tuned to produce the two Higgs eigenstates H_u and H_d of the MSSM.

The job of fixing the position of each stack of branes on each torus is equivalent to fixing the open-string moduli. D-brane constructions typically have non-chiral open string states present in the low-energy spectrum associated with the D-brane position in the internal space and Wilson lines. This results in adjoint or additional matter in the symmetric and antisymmetric representations unless the open string moduli are completely frozen. These light scalars are not observed and the successful gauge unification in the MSSM would also be spoiled by their presence. While it may be possible to find some scenarios where the problems created by these fields are ameliorated, it is much simpler to eliminate these fields altogether. One way to do this is to construct intersecting D-brane models where the D-branes wrap rigid cycles, which was first explored in [16] and [17] in the context of Type II compactifications on $T^6/(\mathbb{Z}_2 \times \mathbb{Z}'_2)$ which is the only known toroidal background which possesses such rigid cycles.

For $T^6/(\mathbb{Z}_2 \times \mathbb{Z}'_2)$ the twisted homology contains collapsed 3-cycles. There are 16 fixed points, from which arise 16 additional 2-cycles with the topology of $\mathbf{P}^1 \cong S^2$. As a result, there are 32 collapsed 3-cycles for each twisted sector. A $D6$ -brane wrapping collapsed 3-cycles in each of the three twisted sectors will be unable to move away from a particular position on the covering space \mathbf{T}^6 , and thus the 3-cycle will be rigid.

A fractional D-brane wrapping both a bulk cycle as well as the collapsed cycles may be written in the form

$$\Pi_a^F = \frac{1}{4}\Pi^B + \frac{1}{4}\left(\sum_{i,j \in S_\theta^a} \epsilon_{a,ij}^\theta \Pi_{ij,a}^\theta\right) + \frac{1}{4}\left(\sum_{j,k \in S_\omega^a} \epsilon_{a,jk}^\omega \Pi_{jk,a}^\omega\right) + \frac{1}{4}\left(\sum_{i,k \in S_{\theta\omega}^a} \epsilon_{a,ik}^{\theta\omega} \Pi_{ik,a}^{\theta\omega}\right). \quad (114)$$

where the $D6$ -brane is required to run through the four fixed points for each of the twisted sectors. The set of four fixed points may be denoted as S^g for the twisted sector g . The constants $\epsilon_{a,ij}^\theta$, $\epsilon_{a,jk}^\omega$ and $\epsilon_{a,ki}^{\theta\omega}$ denote the sign of the charge of the fractional brane with respect to the fields which are present at the orbifold fixed points. We refer the reader to [17] for a detailed discussion of model building on this background.

Let us consider a local supersymmetric model consisting of three stacks of $D6$ branes wrapping fractional cycles with the bulk wrapping numbers and intersection numbers shown in Table XI. This model is essentially equivalent to the model we have been studying, modulo the fact that the $D6$ branes are now wrapping fractional cycles and there are no longer any flat directions for the open-string moduli. Thus, the positions of the D-branes are frozen since they are unable to move away from the fixed points. Phenomenologically, this is very desirable. First, the existence of the adjoint which results from unstabilized open-string moduli can destroy the gauge-coupling unification and the asymptotic freedom of $SU(3)_C$. Second, fixing the open-string moduli means that there is limited freedom in the values taken by the brane-shift parameters (ϵ_i of the previous section). As we have seen, these parameters play a fundamental role in generating the mass hierarchies between up-type and down-type quarks, and the leptons. In addition, the open-string moduli must be fixed in order to calculate parameters such as μ and $\tan \beta$ which play a very important role in determining the low-energy superpartner spectra and the Yukawa couplings. Finally, instanton induced superpotential couplings may also be very important for addressing issues such as neutrino masses, inflation and supersymmetry breaking. The Euclidean D-branes necessary for calculating such effects must wrap rigid cycles.

In order to have such rigid cycles, we must make a choice of discrete torsion which is related to the sign of the orientifold planes. Namely, in order for the background to have discrete torsion, there must be an odd number of $O6^{(+,+)}$ planes. Thus, the conditions necessary for tadpole cancellation

TABLE XI: D6-brane configurations and bulk intersection numbers for a local left-right model in Type IIA on the $\mathbf{T}^6/(\mathbb{Z}_2 \times \mathbb{Z}'_2)$ orientifold, where the D6-branes are wrapping rigid cycles. Although the bulk intersection numbers are the same for stacks a_1 and a_2 , it should be understood that the cycles wrapped by these stacks go through different fixed points on at least one torus.

	$SU(3)_C \times SU(2)_L \times SU(2)_R \times U(1)_{B-L}$										
	N	$(n^1, l^1) \times (n^2, l^2) \times (n^3, l^3)$	n_S	n_A	b	b'	c	c'	$\epsilon_{ij}^\theta \forall ij$	$\epsilon_{jk}^\omega \forall jk$	$\epsilon_{kl}^{\theta\omega} \forall kl$
a_1	3	$(1, 0) \times (1, -1) \times (1, 1)$	0	0	-3	1	3	-1	-1	-1	1
a_2	1	$(1, 0) \times (1, -1) \times (1, 1)$	0	0	-3	1	3	-1	-1	-1	1
b	2	$(1, 3) \times (1, 0) \times (1, -1)$	0	4	-	-	0	2	1	1	1
c	2	$(1, -3) \times (0, 1) \times (1, -1)$	-8	0	-	-	-	-	1	1	1

depend directly on the choice of discrete torsion, which will then determine what combination of hidden sector branes and/or flux is necessary in order to have a globally consistent model. The hidden sector will also be necessary to cancel twisted-tadpoles associated with the orbifold fixed points.

Of course, in the end, our strategy will be to construct the model in the T-dual picture involving magnetized fractional D-branes, in the context of flux compactifications. Indeed, it is necessary to turn on fluxes in order to stabilize the closed-string moduli. In fact, one such model with an equivalent observable sector as the one we have been studying has been constructed as examples of supersymmetric Type IIA Ads and Type IIB Minkowski flux vacua [36, 39]. The next step would then be to combine these two sources of moduli stabilization into a single construction with both open and closed-string moduli stabilized. Hopefully, we would then be able to uniquely calculate both the Yukawa couplings as well as the superpartner spectra. We are presently working on this, and hope to report on our progress in the near future.

IX. CONCLUSION

We have analyzed in detail a three-family intersecting D6-brane model where gauge coupling unification is achieved at the string scale and where the gauge symmetry can be broken to the Standard Model. In the model, it is possible to calculate the supersymmetry breaking soft terms and obtain the low energy supersymmetric particle spectra within the reach of the LHC. Finally, it is possible to obtain the SM quark masses and CKM mixings and the lepton masses, and the neutrino masses and mixings may be generated via the seesaw mechanism.

Clearly, this model cannot be regarded as being fully realistic until the moduli stabilization issue has been fully addressed. There are many free parameters which have been fixed in order to obtain the desired values for the Yukawa mass matrices and the value of the gauge couplings at the unification scale, although it should be kept in mind that these parameters are tightly constrained and it is not possible to tune them to just any value. In the case of the Yukawa matrices, the free parameters are the Kähler moduli, the brane positions on each torus (open-string moduli) and the specific linear combination of states with which have been identified the two pairs of Higgs eigenstates. Although we have chosen specific values for the moduli fields to obtain agreement with experiments, it may be possible to uniquely predict these values by introducing the most general fluxes. It might also be possible to fix the open string moduli if we require the D-branes wrap rigid cycles. However, it seems likely that the Higgs eigenstates would still need to be fine-tuned.

On the other hand, this does appear to be the first such string-derived model where it is possible to give mass to each family of quarks and leptons. Even if we cannot at present *uniquely* predict these values, it must still be regarded as highly significant in that it is *possible* to come very close to getting correct mass matrices and mixings at the unification scale. This suggests that the model may be a candidate for a phenomenological description of elementary particle physics in much the same way as the MSSM.

It is also very appealing that the tree-level gauge couplings are unified at the string scale, although it is still an open question if the running of the gauge couplings can be maintained all the way down to the electroweak scale. The reason for this is that there are chiral exotic states present in the spectrum which are bifundamentals under the observable and hidden sector gauge groups. We should note that most of these chiral exotic states can be decoupled at the string scale and the rest may be decoupled at an intermediate scale. Even if this were not the case, we have found that the hidden sector gauge interactions will become confining at around 10^7 GeV and 10^{13} GeV respectively, and so states charged under these groups will not be present

in the low-energy spectrum. However, there are exotic states in the spectrum which transform as representations of both the hidden and observable sectors which may effect the RGE running of the gauge couplings, although we do not expect them to effect the running that much. If we are optimistic, then it is possible that these would amount to threshold corrections which might push the unification scale up to the string scale.

If the model does turn out to be a realistic effective description of the observed elementary particle physics, then it should be possible to predict the low-energy superpartner mass spectra from the model. Besides the D-brane wrapping numbers and closed-string moduli, the superpartner spectra depend strongly on the exact way in which supersymmetry is broken. In principle, it should be possible to completely specify the exact mechanism, whether through gaugino condensation in the hidden sector, flux-induced soft terms, or via instanton induced couplings. In the present analysis, we have studied supersymmetry breaking generically via a generic parameterized F-term and have shown that it is possible to constrain the phenomenologically allowed parameter space by imposing experimental limits on the neutralino relic density and mass limits coming from LEP. We have found that the viable parameter space is quite large. Once the experimentally determined superpartner mass spectrum begins to take shape it may be possible to find a choice of F-terms which will correspond to the observed spectrum. It would be very interesting to explore the collider signatures which this model may produce at LHC for the regions of the parameter space which satisfy all phenomenological constraints.

In summary, the model we have studied may produce a realistic phenomenology, once the issue of moduli stabilization has been fully addressed. The model represents the first known intersecting D-brane model for which mass may be given to each generation of quarks and leptons. Furthermore, the supersymmetry breaking soft terms may be studied in the model and may yield realistic superpartner spectra. Certainly, the model and the current theoretical tools are not presently developed to the point where specific predictions for the known fermion masses and superpartner spectrum may be made. However, it is clearly possible for the model to describe the known physics of the Standard Model, as well as potentially describing new physics.

Acknowledgements

This research was supported in part by the Mitchell-Heep Chair in High Energy Physics (CMC), by the Cambridge-Mitchell Collaboration in Theoretical Cosmology and by the Chinese Academy of Sciences under Grant KJCX3-SYW-N2(TL), and by the DOE grant DE-FG03-95-Er-40917.

-
- [1] J. Polchinski and E. Witten, Nucl. Phys. B **460**, 525 (1996) [arXiv:hep-th/9510169].
 - [2] M. Berkooz, M. R. Douglas and R. G. Leigh, Nucl. Phys. B **480**, 265 (1996) [arXiv:hep-th/9606139].
 - [3] C. Bachas, [arXiv:hep-th/9503030].
 - [4] E. Witten, JHEP **9812**, 019 (1998).
 - [5] R. Blumenhagen, L. Görlich, B. Körs and D. Lüst, JHEP **0010**, 006 (2000) [arXiv:hep-th/0007024].
 - [6] C. Angelantonj, I. Antoniadis, E. Dudas and A. Sagnotti, Phys. Lett. B **489**, 223 (2000) [arXiv:hep-th/0007090].
 - [7] R. Blumenhagen, M. Cvetič, P. Langacker and G. Shiu, Ann. Rev. Nucl. Part. Sci. **55**, 71 (2005) [arXiv:hep-th/0502005], and the references therein.
 - [8] M. Cvetič, G. Shiu and A. M. Uranga, Phys. Rev. Lett. **87**, 201801 (2001).
 - [9] M. Cvetič, G. Shiu and A. M. Uranga, Nucl. Phys. B **615**, 3 (2001).
 - [10] M. Cvetič, I. Papadimitriou and G. Shiu, Nucl. Phys. B **659**, 193 (2003) [Erratum-ibid. B **696**, 298 (2004)].
 - [11] M. Cvetič and I. Papadimitriou, Phys. Rev. D **67**, 126006 (2003).
 - [12] M. Cvetič, T. Li and T. Liu, Nucl. Phys. B **698**, 163 (2004).
 - [13] M. Cvetič, P. Langacker, T. Li and T. Liu, Nucl. Phys. B **709**, 241 (2005).
 - [14] C.-M. Chen, G. V. Kraniotis, V. E. Mayes, D. V. Nanopoulos and J. W. Walker, Phys. Lett. B **611**, 156 (2005); Phys. Lett. B **625**, 96 (2005).
 - [15] C.-M. Chen, T. Li and D. V. Nanopoulos, Nucl. Phys. B **732**, 224 (2006).
 - [16] E. Dudas and C. Timirgaziu, Nucl. Phys. B **716**, 65 (2005) [arXiv:hep-th/0502085].
 - [17] R. Blumenhagen, M. Cvetič, F. Marchesano and G. Shiu, JHEP **0503**, 050 (2005) [arXiv:hep-th/0502095].
 - [18] C. M. Chen, V. E. Mayes and D. V. Nanopoulos, Phys. Lett. B **648**, 301 (2007) [arXiv:hep-th/0612087].
 - [19] M. Cvetič, P. Langacker and G. Shiu, Phys. Rev. D **66**, 066004 (2002); Nucl. Phys. B **642**, 139 (2002).
 - [20] M. Cvetič, P. Langacker and J. Wang, Phys. Rev. D **68**, 046002 (2003).
 - [21] R. Blumenhagen, L. Görlich and T. Ott, JHEP **0301**, 021 (2003); G. Honecker, Nucl. Phys. B **666**, 175 (2003); G. Honecker and T. Ott, Phys. Rev. D **70**, 126010 (2004) [Erratum-ibid. D **71**, 069902 (2005)].
 - [22] R. Blumenhagen, M. Cvetič and T. Weigand, arXiv:hep-th/0609191.
 - [23] L. E. Ibanez and A. M. Uranga, JHEP **0703**, 052 (2007).
 - [24] M. Cvetič, R. Richter and T. Weigand, arXiv:hep-th/0703028.
 - [25] L. E. Ibanez, A. N. Schellekens and A. M. Uranga, arXiv:0704.1079 [hep-th].
 - [26] S. Kachru, M. B. Schulz and S. Trivedi, JHEP **0310**, 007 (2003) [arXiv:hep-th/0201028]; R. Blumen-

- hagen, D. Lüüst and T. R. Taylor, Nucl. Phys. B **663**, 319 (2003) [arXiv:hep-th/0303016].
- [27] T. W. Grimm and J. Louis, Nucl. Phys. B **718**, 153 (2005) [arXiv:hep-th/0412277]; G. Villadoro and F. Zwirner, JHEP **0506**, 047 (2005) [arXiv:hep-th/0503169].
- [28] J. F. G. Cascales and A. M. Uranga, JHEP **0305**, 011 (2003).
- [29] F. Marchesano and G. Shiu, Phys. Rev. D **71**, 011701 (2005); JHEP **0411**, 041 (2004).
- [30] M. Cvetič and T. Liu, Phys. Lett. B **610**, 122 (2005).
- [31] M. Cvetič, T. Li and T. Liu, Phys. Rev. D **71**, 106008 (2005).
- [32] J. Kumar and J. D. Wells, JHEP **0509**, 067 (2005).
- [33] C.-M. Chen, V. E. Mayes and D. V. Nanopoulos, Phys. Lett. B **633**, 618 (2006).
- [34] R. Blumenhagen, B. Kors, D. Lust and S. Stieberger, arXiv:hep-th/0610327.
- [35] P. G. Camara, A. Font and L. E. Ibanez, JHEP **0509**, 013 (2005).
- [36] C.-M. Chen, T. Li and D. V. Nanopoulos, Nucl. Phys. B **740**, 79 (2006).
- [37] C.-M. Chen, T. Li and D. V. Nanopoulos, Nucl. Phys. B **751**, 260 (2006).
- [38] C.-M. Chen, T. Li, V. E. Mayes and D. V. Nanopoulos, arXiv:hep-th/0703280.
- [39] C. M. Chen, T. Li, Y. Liu and D. V. Nanopoulos, arXiv:0711.2679 [hep-th].
- [40] C. L. Bennett *et al.* [WMAP Collaboration], Astrophys. J. Suppl. **148**, 1 (2003) [arXiv:astro-ph/0302207].
- [41] D. N. Spergel *et al.* [WMAP Collaboration], Astrophys. J. Suppl. **148**, 175 (2003) [arXiv:astro-ph/0302209].
- [42] R. Blumenhagen, B. K rs, D. Lüüst and T. Ott, Nucl. Phys. B **616**, 3 (2001) [arXiv:hep-th/0107138].
- [43] D. Cremades, L. E. Ib   ez and F. Marchesano, JHEP **0207**, 009 (2002) [arXiv:hep-th/0201205].
- [44] G. Shiu and S. H. H. Tye, Phys. Rev. D **58**, 106007 (1998) [arXiv:hep-th/9805157].
- [45] D. Lüüst and S. Stieberger, [arXiv:hep-th/0302221].
- [46] I. Antoniadis, E. Kiritsis and T. N. Tomaras, Phys. Lett. B **486**, 186 (2000) [arXiv:hep-ph/0004214]; R. Blumenhagen, D. Lust and S. Stieberger, JHEP **0307**, 036 (2003) [arXiv:hep-th/0305146].
- [47] D. Cremades, L. E. Ib   ez and F. Marchesano, JHEP **0307**, 038 (2003) [arXiv:hep-th/0302105].
- [48] M. Cvetič and I. Papadimitriou, Phys. Rev. D **68**, 046001 (2003) [Erratum-ibid. D **70**, 029903 (2004)] [arXiv:hep-th/0303083].
- [49] B. K rs and P. Nath, Nucl. Phys. B **681**, 77 (2004) [arXiv:hep-th/0309167].
- [50] D. Lüüst, P. Mayr, R. Richter and S. Stieberger, Nucl. Phys. B **696**, 205 (2004) [arXiv:hep-th/0404134].
- [51] Y. Kawamura, T. Kobayashi and T. Komatsu, Phys. Lett. B **400**, 284 (1997) [arXiv:hep-ph/9609462].
- [52] A. Brignole, L. E. Ibanez and C. Munoz, Nucl. Phys. B **422**, 125 (1994) [Erratum-ibid. B **436**, 747 (1995)] [arXiv:hep-ph/9308271]; [arXiv:hep-ph/9707209].
- [53] R. Blumenhagen, D. Lust and S. Stieberger, JHEP **0307**, 036 (2003) [arXiv:hep-th/0305146].
- [54] J. R. Ellis, J. L. Lopez and D. V. Nanopoulos, Phys. Lett. B **247**, 257 (1990).

- [55] K. Benakli, J. R. Ellis and D. V. Nanopoulos, Phys. Rev. D **59**, 047301 (1999) [arXiv:hep-ph/9803333].
- [56] J. R. Ellis, V. E. Mayes and D. V. Nanopoulos, Phys. Rev. D **70**, 075015 (2004) [arXiv:hep-ph/0403144].
- [57] J. R. Ellis, V. E. Mayes and D. V. Nanopoulos, Phys. Rev. D **74**, 115003 (2006) [arXiv:astro-ph/0512303].
- [58] G. L. Kane, P. Kumar, J. D. Lykken and T. T. Wang, Phys. Rev. D **71**, 115017 (2005) [arXiv:hep-ph/0411125].
- [59] A. Font and L. E. Ibanez, JHEP **0503**, 040 (2005) [arXiv:hep-th/0412150].
- [60] A. Djouadi, J. L. Kneur and G. Moultaka, Comput. Phys. Commun. **176**, 426 (2007) [arXiv:hep-ph/0211331].
- [61] G. Belanger, F. Boudjema, A. Pukhov and A. Semenov, Comput. Phys. Commun. **174**, 577 (2006).
- [62] G. Aldazabal, S. Franco, L. E. Ibanez, R. Rabadan and A. M. Uranga, JHEP **0102**, 047 (2001) [arXiv:hep-ph/0011132].
- [63] N. Chamoun, S. Khalil and E. Lashin, Phys. Rev. D **69**, 095011 (2004) [arXiv:hep-ph/0309169].
- [64] T. Higaki, N. Kitazawa, T. Kobayashi and K. j. Takahashi, Phys. Rev. D **72**, 086003 (2005) [arXiv:hep-th/0504019].
- [65] G. Ross and M. Serna, arXiv:0704.1248 [hep-ph].
- [66] H. Fusaoka and Y. Koide, Phys. Rev. D **57**, 3986 (1998) [arXiv:hep-ph/9712201].
- [67] Ching-Ming Chen, Tianjun Li, V. E. Mayes, James Maxin, D. V. Nanopoulos, in preparation.